# Identification of USP7 as an essential component to maintain integrity and function of non-canonical PRC1.1 in leukemia

Henny Maat[1], Jennifer Jaques[1], Aida Rodríguez López[1], Marcel P. de Vries[2,3], Chantal Gravesteijn[1], Annet Z. Brouwers-Vos[1], Gerwin Huls[1], Edo Vellenga[1], Vincent van den Boom[1] and Jan Jacob Schuringa[1,*].

[1]Department of Experimental Hematology, Cancer Research Center Groningen, University Medical Center Groningen, University of Groningen, Hanzeplein 1, 9713 GZ Groningen, The Netherlands;

[2]Department of Pharmacy, Interfaculty Mass Spectrometry Center, University of Groningen, A. Deusinglaan 1, 9713 AV Groningen, The Netherlands;

[3]Department of Pediatrics, Center for Liver, Digestive, and Metabolic Diseases, University Medical Center Groningen, University of Groningen, Hanzeplein 1, 9713 GZ Groningen, The Netherlands

[*]Correspondence: j.j.schuringa@umcg.nl. Department of Experimental Hematology, Medical Center Groningen, University of Groningen, Hanzeplein 1, DA13, 9713 GZ Groningen, The Netherlands.

**ABSTRACT**

Polycomb proteins are essential epigenetic regulators of gene transcription. KDM2B, the chromatin-binding moiety of non-canonical PRC1.1, is critically important for human leukemias. Here, we investigated the complete interactome of KDM2B in human leukemic cells and identified that the deubiquitinase USP7 is an essential component of PRC1.1 and required for its stability and function. USP7 inhibition results in disassembly of the PRC1.1 complex and consequently loss of binding to its target loci. PRC1.1 can be associated with active loci and loss of PRC1.1 binding coincided with loss of H2AK119ub, reduced H3K27ac levels and reduced gene transcription, whereas H3K4me3 levels remained unaffected. Survival was reduced in (primary) acute myeloid leukemia cells in both cycling as well as quiescent populations upon USP7 inhibition, also independent of the USP7-MDM2-p53 axis. Finally, we evaluated the efficacy of USP7 inhibition *in vivo* and find that progression of MLL-AF9-induced leukemia is delayed, although in a niche-dependent manner.

**INTRODUCTION**

Regulation of gene transcription is carefully coordinated to control stem cell self-renewal and differentiation. Polycomb group (PcG) proteins are important epigenetic regulators and critically involved in controlling gene transcription by mediating post-translational modifications of histone proteins and chromatin remodeling (Kouzarides, 2007; Mas & Di, 2016; Simon & Kingston, 2013). Genome-wide analyses of Polycomb target genes revealed the occupancy of PcG proteins at promoters of genes regulating cell fate, highlighting their importance for proper lineage specification (Boyer et al., 2006; Bracken, Dietrich, Pasini, Hansen, & Helin, 2006; T. I. Lee et al., 2006). Yet, how PcG proteins are recruited, recognize their target genes and regulate gene expression still remains poorly understood. Understanding these processes is important since deregulation of PcG proteins frequently contributes to cancer and hematopoietic malignancies, like leukemia (Bracken & Helin, 2009; D. Hu & Shilatifard, 2016; Piunti & Shilatifard, 2016).

44 PcG proteins form multi-protein chromatin modifying complexes of which Polycomb Repressive
45 Complex 1 (PRC1) and 2 (PRC2) are best characterized (Simon & Kingston, 2009). PRC2, by means of
46 EZH1/EZH2, catalyzes the trimethylation of histone H3 on lysine 27 (H3K27me3) which can be
47 recognized by the chromodomain protein (CBX) of the canonical PRC1 complex (Cao et al., 2002;
48 Kirmizis et al., 2004; Kuzmichev, Nishioka, Erdjument-Bromage, Tempst, & Reinberg, 2002). PRC1
49 monoubiquitinates histone H2A on lysine 119 (H2AK119ub) via either one of the two E3 ligases
50 RING1A/1B (de Napoles et al., 2004; H. Wang et al., 2004). Proteome analysis has identified the
51 composition of six major PRC1 complexes that all contain RING1A or RING1B and distinguished by the
52 presence of one of the six PCGF proteins (PCGF1-6) (Gao et al., 2012; van den Boom et al., 2016).
53 Canonical PRC1 complexes contain either PCGF2 or PCGF4 and one of the CBX paralogs
54 (CBX2/4/6/7/8), PHC (1/2/3) and SCML1/SCML2/SCMH1 subunits. Non-canonical PRC1 complexes
55 lack a CBX subunit and instead contain RYBP or YAF2 which all three compete for the same binding
56 site of RING1B (Gao et al., 2012; R. Wang et al., 2010). The exact function of individual subunits in the
57 PRC1 complex is not fully understood, though it is suggested that they are involved in maintaining
58 the integrity of the complex, in providing or controlling enzymatic activity or in targeting to
59 chromatin. For example, the H2AK119 E3 ligase activity is enhanced by the dimerization of RING1A/B
60 with either PCGF2 or PCGF4 (Buchwald et al., 2006; Cao, Tsukada, & Zhang, 2005; Elderkin et al.,
61 2007) or can be stimulated by the PCGF1-RYBP/YAF2 interaction in the case of non-canonical PRC1.1
62 (Gao et al., 2012; Rose et al., 2016). A shRNA approach for individual PRC1 subunits in hematopoietic
63 stem cells revealed a lack of functional redundancy, suggesting unique functions of distinct PRC1
64 complexes (van den Boom et al., 2013) and indeed PRC1 complex composition changes upon lineage
65 specification (Morey et al., 2015).
66 To better understand the function of PRC1 complexes in human leukemias, we recently identified an
67 essential role for non-canonical PRC1.1 proteins (van den Boom et al., 2016). PRC1.1 was first
68 identified by the purification of the BCOR protein, which was found to interact with RING1A/B, RYBP,
69 PCGF1, SKP1 and KDM2B (Gearhart, Corcoran, Wamstad, & Bardwell, 2006; Sanchez et al., 2007). A

70 potential oncogenic role of PRC1.1 is underlined by the fact that KDM2B is overexpressed in
71 leukemias, breast and pancreatic cancers where it functions as an oncogene, conversely knockdown
72 of KDM2B abrogated tumorigenicity (Andricovich, Kai, Peng, Foudi, & Tzatsos, 2016; He, Nguyen, &
73 Zhang, 2011; Kottakis et al., 2014; Ueda et al., 2015; van den Boom et al., 2016).
74 Via the ZF-CxxC domain of KDM2B, PRC1.1 is targeted to non-methylated CpG islands genome-wide
75 and contributes to PRC1.1 recruitment (Blackledge et al., 2014; Farcas et al., 2012; He et al., 2013;
76 van den Boom et al., 2016; Wu, Johansen, & Helin, 2013). The PRC1.1 complex assembles around a
77 core PCGF1-RING1B dimer (Junco et al., 2013; Rose et al., 2016; Wong et al., 2016). While Polycomb-
78 mediated silencing by canonical PRC1 and PRC2 complexes is thought to maintain compacted
79 chromatin, which is inhibitory to transcription (Francis, Kingston, & Woodcock, 2004; Muller &
80 Verrijzer, 2009), less is known about the function of PRC1.1 on gene transcription. In mouse
81 embryonic stem cells (mESCs) and mouse embryonic fibroblasts it is suggested that KDM2B functions
82 together with PRC2 to repress lineage-specific genes (Blackledge et al., 2014; He et al., 2013; Tzatsos,
83 Pfau, Kampranis, & Tsichlis, 2009). On the other hand, Boulard and colleagues find more DNA
84 methylation in KDM2B null mESC at CpG islands co-occupied by PRC2, suggesting that KDM2B keeps
85 promoters in an activated non-methylated state (Boulard, Edwards, & Bestor, 2015). We and others
86 have shown that PRC1.1/KDM2B can also be targeted to sites independent of PRC2/H3K27me3 and
87 notably is associated with 'permissive' or active chromatin suggested by the occupancy of H3K4me3,
88 H3K36me3, RNAPII (S5P) and H3K27ac (Engelen et al., 2015; Liang, He, & Zhang, 2012; Tavares et al.,
89 2012; van den Boom et al., 2016).
90 A better understanding of PRC1.1 function is required in order to understand its role in gene
91 regulation and to explore possibilities to target PRC1.1 in human diseases such as leukemia. Here, we
92 investigated KDM2B/PRC1.1 in more detail with the aim to identify alternative approaches to target
93 the non-canonical PRC1.1 complex in human leukemic cells. LC-MS/MS-based proteome studies were
94 used to investigate the complete interactome of KDM2B in human leukemic cells and we identified
95 that the deubiquitinase USP7 is an essential component of PRC1.1 and is required to maintain its

integrity and function. As a consequence of inhibiting USP7 deubiquitinase activity the PRC1.1 complex disassembles and loses binding to chromatin, with a concomitant reduction in gene expression of target loci. Furthermore, our data show that USP7 is essential for leukemic cells and suggests that targeting of USP7 might provide an alternative therapeutic approach for leukemia.

## RESULTS

### Identification of the deubiquitinase USP7 as a subunit of PRC1.1

We recently identified KDM2B as a critically important factor for the survival of human leukemic stem cells (van den Boom et al., 2016). Therefore, we set out to study the KDM2B interactome in detail in leukemic cells. Human K562 cells were transduced with KDM2B-EGFP followed by anti-EGFP pull outs and LC-MS/MS analysis to identify interacting proteins. Thus, 406 KDM2B-interacting proteins were identified involved in cellular processes like DNA/chromatin binding, protein binding, RNA binding and RNA polymerase activity (Figure 1 – source data 1, Figure 1A). Gene Ontology analyses revealed that this list contained proteins that associated with rRNA processing, mRNA splicing, translation, mRNA processing, positive regulation of gene expression and DNA damage response (Figure 1B). The most abundant KDM2B interaction partners were non-canonical PRC1.1 proteins (Figure 1C), including the ubiquitin-specific protease 7 (USP7). Since inhibitors are available that inhibit its deubiquitinase activity, we questioned whether inhibition of USP7 could be an alternative way to target leukemic stem cells, in part via inhibition of PRC1.1 and therefore we continued to study the role of USP7 in further detail. To validate the interaction of USP7 with PRC1.1 proteins, besides KDM2B, we also performed EGFP pull outs on nuclear extracts of stable K562 cell lines expressing PCGF1-EGFP and EGFP-RING1B followed by LC-MS/MS analysis (Figure 1 – source data 2). Figure 1D shows the spectral counts (MS/MS counts) corrected for expected peptides based on *in silico* protein digests. Clearly, USP7 was found to interact directly with KDM2B, PCGF1 and RING1B and all other PRC1.1 proteins were co-purified. In addition, Western blots of independent pull outs on canonical PRC1 (PCGF2, PCGF4, CBX2) and non-canonical PRC1.1 (PCGF1, RING1B) were

122 performed using antibodies against USP7 and RING1B (Figure 1E). As expected, RING1B precipitated
123 with both PRC1 and PRC1.1 proteins. The interaction of USP7 with RING1B and PCGF1 was confirmed
124 by Western blot while less interaction was observed with the canonical PRC1 proteins PCGF2, PCGF4
125 or CBX2 (Figure 1E).
126
127 **USP7 inhibition results in disassembly of the PRC1.1 complex**
128 Deubiquitinating enzymes (DUBs) exert a variety of important cellular functions, including the control
129 over protein stabilization or degradation, protein localization, protein activity or by modulating
130 protein-protein interactions (Leznicki & Kulathu, 2017). We therefore questioned whether inhibition
131 of the deubiquitinase USP7 might affect PRC1.1 stability and function. P22077 (1-(5-((2,4-
132 difluorophenyl)thio)-4-nitrothiophen-2-yl)ethanone) has been identified as a selective inhibitor of
133 USP7, as well as USP47, using activity-based chemical proteomics (Altun et al., 2011; Tian et al.,
134 2011). In general, DUB inhibitors increase overall protein polyubiquitination (Altun et al., 2011).
135 Similarly, we observed accumulation of polyubiquitinated proteins in our EGFP-RING1B and PCGF1-
136 EGFP K562 cells treated for 24h with P22077 (Figure 2A). Next, we investigated the effect of USP7
137 inhibition on the stability of PRC1.1. EGFP pull outs were performed on nuclear extracts from K562
138 PCGF1-EGFP and EGFP-RING1B cells treated with DMSO or P22077 followed by LC/MS-MS analysis
139 (Figure 2B, Figure 2 – source data 1). Volcano plots were generated using label-free quantification
140 (LFQ) intensities of potential interactors of EGFP-RING1B (left) and PCGF1-EGFP (right) plotted as fold
141 change difference (control/USP7i) against significance (t-test p-value). Interactions with several
142 PRC1.1 proteins, highlighted in orange, were significantly reduced in both EGFP-RING1B and PCGF1-
143 EGFP pull outs as a consequence of USP7 inhibition (Figure 2B). The ubiquitin protein, UBB, was
144 enriched in both PCGF1-EGFP and EGFP-RING1B pull outs upon P22077 treatment, suggesting that
145 these proteins or other Polycomb interaction proteins might be more ubiquitinated upon USP7
146 inhibition. In addition we analysed the intensity-based absolute quantification (iBAQ) values, as a
147 measure for protein abundance, relative to either RING1B or PCGF1 and normalized to control pull

148 outs (Figure 2C). Similarly, these data demonstrated a clear reduced interaction of PRC1.1 proteins
149 with RING1B and PCGF1 after P22077 treatment. Independent EGFP pull outs performed on PCGF1-
150 EGFP and EGFP-RING1B cell lines further confirmed that USP7 inhibition indeed resulted in reduced
151 interaction of PCGF1-EGFP with endogenous RING1B and EGFP-RING1B with endogenous PCGF1
152 (Figure 2D). Importantly, input samples did not reveal loss of protein stability and also the expression
153 of EGFP-RING1B and PCGF1-EGFP was not affected as quantified by FACS analysis (Figure 2E). Taken
154 together these data indicate that USP7 is essential for PRC1.1 complex integrity.
155
156 **PRC1.1 chromatin binding relies on functional USP7 deubiquitinase activity**
157 To determine the functional consequences of disassembly of the PRC1.1 complex upon USP7
158 inhibition, we performed ChIP to investigate whether PRC1.1 would still be recruited to target loci.
159 Previously, we identified PRC1 and PRC1.1 target loci by ChIP-seq for PCGF1/2/4, CBX2, RING1A/1B,
160 KDM2B, H2AK119ub and H3K27me3 in the leukemic cell line K562 (van den Boom et al., 2016). Here,
161 ChIP-qPCRs were performed for KDM2B, PCGF1 and RING1B, the core PRC1.1 subunits, on a selected
162 set of loci in the absence or presence of P22077 (30 µM). Inhibition of USP7 resulted in a complete
163 loss of KDM2B binding, with concomitant strong reductions in PCGF1 and RING1B chromatin binding
164 (Figure 3A). Importantly, USP7 inhibition did not result in reduced protein levels of KDM2B, PCGF1 or
165 RING1B (Figure 2D/2E and data not shown). Since RING1B mediates H2AK119 ubiquitination we then
166 analysed the levels of this histone modification upon USP7 inhibition. Similarly, H2AK119ub was lost
167 from PRC1.1 target loci. Since USP7 does not target H2AK119 directly, these data suggest that USP7
168 inhibition severely impacts on PRC1.1 chromatin binding and as a consequence H2AK119ub levels.
169 Since non-canonical PRC1.1 can be recruited to active loci in leukemic cells, we also investigated the
170 levels of H3K4me3, but no changes were observed on this histone mark upon USP7 inhibition, further
171 highlighting that not all posttranslational histone modifications are affected as a consequence of
172 treatment (Figure 3B). To test whether the loss of H2AK119ub would indeed be the result of
173 impaired *de novo* ubiquitination by either one of the two E3 ligases RING1A/1B, cells were cross-

174 linked at 4h, 8h and 16h followed by a ChIP for H2AK119ub, KDM2B and RING1B (Figure 3C). The
175 time-dependent loss of H2AK119ub coincided with a loss of KDM2B and RING1B binding at the same
176 target loci, strongly suggesting that loss of *de novo* ubiquitination underlies these observations.
177 Again, H3K4me3 levels remained unaffected, while H3K27ac levels were reduced upon USP7
178 inhibition indicative for reduced transcriptional activity at these loci (Figure 3D).
179
180 **USP7 inhibition leads to downregulation of several PRC1.1 active target genes**
181 Given that USP7 inhibition severely impaired PRC1.1 occupancy to several target loci we investigated
182 whether this would also affect the expression of PRC1.1 target genes in leukemic cells. RNA-seq was
183 performed to compare gene expression in DMSO or USP7 inhibitor treated K562 cells (P22077, 30
184 µM) for 4h, 8h, 16h and 24h. Since PRC1.1 can be associated with active genes in leukemic cells we
185 focused on the genes that were downregulated upon USP7 inhibition. In total 297 genes were
186 downregulated more than 2 fold after 24h of USP7 inhibition (Figure 4 – source data 1). Since USP7
187 has also PRC1.1 independent functions, for instance by controlling MDM2/p53 (Li, Brooks, Kon, & Gu,
188 2004), we then analysed whether downregulated genes overlapped with previously identified PRC1.1
189 (Figure 4A, Figure 4 – source data 2). Twenty-four percent of these genes overlapped with PRC1.1
190 targets. Gene Ontology (GO) analysis revealed that this set was enriched for GO terms like
191 transcription, regulation of gene expression and chromatin modification, while PRC1.1 independent
192 downregulated genes were enriched for GO terms like mRNA splicing, protein folding and protein
193 polyubiquitination (Figure 4B). ChIP-seq profiles of TOP2B, SIN3A, CHD1 and MYC are shown in Figure
194 4C as representative examples for PRC1.1 target genes. The tracks show clear binding of PCGF1,
195 RING1A/1B and KDM2B and little occupancy of canonical PRC1 proteins (PCGF2, PCGF4, CBX2). These
196 loci were also enriched for H2AK119ub and active chromatin marks H3K4me3, H3K36me3, RNAPII
197 and H3K27ac but devoid of the repressive mark H3K27me3. Loss of PRC1.1 binding was confirmed by
198 ChIP-qPCRs for KDM2B, PCGF1 and RING1B on these 4 loci (Figure 4D). Again, a concomitant loss of
199 H2AK119ub and H3K27ac marks was seen, without any alterations in H3K4me3. Subsequently, the

200 observed downregulation based on RNA-seq data was validated by independent quantitative RT-
201 PCRs (Figure 4E). In the majority of cases we observed that loss of PRC1.1 binding strongly correlated
202 with loss of gene expression, with only a few exceptions. For instance PKM, KIF21B and SLC25A22
203 were not downregulated despite a clear loss of PRC1.1 binding at these loci, suggesting that
204 transcription is controlled by additional mechanisms as well. Taken together, these data suggest that
205 the presence of PRC1.1 is required to maintain the transcriptional activity of several target genes.
206
207 **Both quiescent and cycling primary AML cell populations are sensitive towards USP7 inhibition**
208 To study the functional consequences of USP7 inhibition, we tested P22077 on the AML cell lines
209 MOLM-13, NB4, KG1a, K562 and HL60. USP7 inhibition severely impaired cell growth in all tested
210 AML cell lines (Figure 5A) associated with increased apoptosis. Also cell lines that do not express
211 functional p53 (HL60 and K562) showed sensitivity, indicating that at least in those cell lines the
212 effect of P22077 was independent of p53 (Figure 5 – source data 1). Next, we assessed whether USP7
213 inhibition also affected the survival of primary AML cells. The long-term proliferation of primary AML
214 $CD34^+$ cells (n=3) on MS5 co-culture was clearly reduced upon USP7 inhibition (Figure 5B). Patient
215 characteristics are shown in Figure 5 – source data 1. With current therapies for leukemia patients
216 the majority of the blast population is readily eradicated, while the rare quiescent population of
217 leukemic stem cells is more difficult to target. To examine the effects of USP7 inhibition on both
218 cycling as well as quiescent ($G_0$) cells, we performed Hoechst/PyroninY stainings. AML 2 was
219 characterized by a large $CD34^+/CD38^+$ population that is high in cycling activity, while the
220 $CD34^+/CD38^-$ population is predominantly in $G_0$ (Figure 5C). In both populations, the $G_0$ fraction was
221 equally or even more efficiently targeted by P22077 compared to the cycling fraction, indicating that
222 cycling cells are not necessarily more sensitive than quiescent cells. AML3 was low in $CD34^+$ and
223 therefore we gated on the whole blast population which also showed that both quiescent and cycling
224 cells were sensitive for P22077 (Figure 5D).
225

226 **Evaluation of USP7 inhibition in xenograft leukemia mouse model**

227 Next, we evaluated the effect of USP7 inhibition in our human CB MLL-AF9 xenograft mouse model
228 (Figure 6A) (Horton et al., 2013; Sontakke et al., 2016). Importantly, these lymphoid MLL-AF9 cells
229 grown on a co-culture of MS5 *in vitro* were sensitive towards USP7 inhibition (Figure 6 – figure
230 supplement 1). Here 5 x $10^4$ MLL-AF9 leukemic cells, from a primary leukemic mouse, were
231 intravenously (IV) injected into secondary recipients (n=11). Three weeks after injection 10/11 mice
232 showed engraftment of MLL-AF9 $EGFP^+/CD45^+/CD19^+$ cells in peripheral blood (Figure 6B).
233 Subsequently, mice were divided into two groups that were treated either with DMSO as control
234 (n=5) or 20 mg/kg P22077 (n=6) via intraperitoneal (IP) injections. Peripheral blood chimerism levels
235 were monitored by regular blood sample analysis and mice were sacrificed when chimerism levels in
236 the blood exceeded 40%. Mice were treated daily starting four weeks post-transplant (indicated with
237 the arrow, Figure 6C). Two-and-a-half weeks after starting treatment, chimerism levels were
238 significantly lower in P22077-treated mice compared to DMSO (Figure 6B and 6C). The chimerism
239 levels for DMSO treated mice rapidly increased to 44% (average) within 6 weeks after injection,
240 whereas the chimerism levels of P22077 treated mice were around 25% on average. Notably, 3/6
241 mice gave a better response to USP7 inhibition with lower chimerism levels of 18.3, 16.8 and 12%
242 respectively at day 46 (Figure 6B). Upon treatment we followed the mice for some additional weeks
243 and within 60 days all control mice exceeded 40% chimerism in the blood, indicative for a full blown
244 leukemia and were sacrificed (Figure 6C and D). Bone marrow, spleen and liver analyses showed high
245 levels (>90%) of chimerism (data not shown). USP7 inhibition delayed leukemia development and in
246 particular in two mice a clear response to USP7 inhibition was observed and chimerism levels
247 remained relatively stable between day 56-67 post-transplant, although ultimately mice did develop
248 MLL-AF9 induced leukemia after day 77 (Figure 6D).

249 Since the efficacy of USP7 inhibition *in vitro* in AML cell lines and patient samples was rather high, in
250 contrast to what we observed *in vivo* in our xenograft mouse model, we hypothesized that the bone
251 marrow niche could potentially play a protective role in the survival of leukemic cells and dampen

252 the response to therapeutic agents (Greim et al., 2014; Karjalainen et al., 2017; Parmar et al., 2011).
253 Therefore we evaluated the efficacy of USP7 inhibition in a direct comparison of CB MLL-AF9 cells
254 grown in liquid culture or in a co-culture setting on murine MS5 bone marrow stromal cells. In both
255 settings P22077 impaired cell growth, but the efficacy was much higher in liquid culture conditions
256 (Figure 6E). Loss of KDM2B binding to PRC1.1 target loci was confirmed by ChIP-qPCRs, both under
257 liquid culture and MS5 co-culture conditions, although we did note that the efficacy was somewhat
258 higher under liquid culture conditions (Figure 6F).
259
260 **DISCUSSION**
261 In this study, we reveal that the deubiquitinase USP7 is an essential component of non-canonical
262 PRC1.1 in leukemia and is required for its stability and function. Inhibiting USP7 deubiquitinase
263 activity, by P22077 treatment, resulted in disassembly of the PRC1.1 complex. Consequently,
264 recruitment of the PRC1.1 complex to target loci was heavily lost coinciding with the loss of its
265 H2AK119ub catalytic activity. This causes repression of a subset of transcriptionally active PRC1.1
266 target genes and corresponds with a reduction in H3K27ac, highlighting an essential function for
267 PRC1.1 in maintaining gene transcription. Furthermore, USP7 inhibition strongly impaired leukemic
268 cell growth *in vitro* and delayed MLL-AF9 induced leukemia *in vivo*, although in a niche-dependent
269 manner.
270 The non-canonical PRC1.1 complex consists of several Polycomb proteins and although we begin to
271 learn more about the function of some of the individual proteins within the complex, the role that
272 others fulfill remains far from completely understood. PRC1.1 is recruited to non-methylated CpG
273 islands via KDM2B and a single point mutation in the ZF-CxxC domain (K643A) of KDM2B has been
274 shown to prevent this interaction (Farcas et al., 2012; He et al., 2013; Wu et al., 2013). The H2AK119
275 E3 ubiquitin ligase activity of both canonical PRC1.2/1.4 and non-canonical PRC1.1 is mediated by
276 RING1A/1B proteins and is supported by the dimerization with one of the PCGFs (PCGF1-6) (Dou,
277 Buetow, Sibbet, Cameron, & Huang, 2012; Endoh et al., 2008; Taherbhoy, Huang, & Cochran, 2015).

278 For example, non-canonical PCGF1/3/5/6-RING1 heterodimers show much higher E3 ligase activity
279 than canonical PCGF2/4-RING1 heterodimers (Taherbhoy et al., 2015). This difference possibly lies in
280 a structural difference in PCGF helix α3 residues between canonical and non-canonical PCGFs which
281 may limit ubiquitin transfer by the RING1 dimer. Furthermore, the interaction of RYBP/YAF2 with the
282 PCGF1-RING1B core dimer increased the relative H2AK119 E3 ligase activity of PRC1.1 in an *in vitro*
283 assay (Rose et al., 2016). KDM2B and BCOR contributed little or nothing to this activity.
284 A role for the deubiquitinase USP7 within PRC1.1 was suggested since USP7 stably interacts with
285 PRC1.1 proteins, KDM2B, PCGF1 and RING1B (Figure 1). Sánchez and colleagues first identified the
286 ubiquitin protease USP7 as an interactor of RING1B (Sanchez et al., 2007). Then, USP7 was also
287 identified in proteomics analysis of PCGF1, RYBP, YAF2 and RING1A/B pullouts (Gao et al., 2012; van
288 den Boom et al., 2016). Previously, USP7 has been shown to be associated with the canonical PRC1
289 protein BMI1 (PCGF4) and potentially also with MEL18 (PCGF2), although Lecona and colleagues
290 suggested that USP7 interacts directly with SCML2 and thereby bridges the interaction with PRC1.4
291 (Lecona, Narendra, & Reinberg, 2015; Maertens, El Messaoudi-Aubert, Elderkin, Hiom, & Peters,
292 2010). Similar to Gao and colleagues (Gao et al., 2012) however, in our canonical PCGF2, PCGF4 and
293 CBX2 proteome analyses we found little or no interaction with USP7 (van den Boom et al., 2016). We
294 did notice that several canonical RING1B-Polycomb interactions were also reduced upon USP7
295 inhibition, including CBX2/4/8, SCML2 and SCMH1, though the interaction with PCGF2 and PCGF4
296 was not affected. This might also suggest that USP7 impacts on PRC1 protein stability, although
297 further studies are required to clarify these issues. In line with that notion, a recent paper
298 demonstrated that another deubiquitinase, USP26, controls the stability of CBX4 and CBX6 and
299 thereby affects the complex composition of PRC1 during ESC reprogramming (Ning et al., 2017).
300 Maertens and colleagues demonstrated that also USP11 interacts with PRC1 proteins and affects the
301 stability of BMI1 (Maertens et al., 2010). Thus, DUBs reveal an interesting role on Polycomb stability
302 and complex composition.

303 Based on our observations, the complex composition of PRC1.1 is affected upon USP7 inhibition. This
304 suggest that controlling ubiquitin levels of Polycomb proteins is important for the integrity of the
305 protein-protein interactions within PRC1.1 and its chromatin binding. Upon USP7 inhibition an overall
306 increase in protein ubiquitination was observed (Figure 2). Importantly, USP7 inhibition did not lead
307 to degradation of PCGF1 or RING1B, allowing us to conclude that USP7 controls protein-protein
308 interactions rather than proteasomal degradation. In line with that notion, overexpression of USP7
309 has been shown to deubiquitinate RING1B thereby stabilizing RING1B and preventing it from
310 proteasomal degradation (de, Zaaroor-Regev, & Ciechanover, 2010). Furthermore, RING1B self-
311 ubiquitination is required for its ligase activity on histone H2A (Ben-Saadon, Zaaroor, Ziv, &
312 Ciechanover, 2006). This is supported by the observation that H2AK119ub is lost upon USP7
313 inhibition, most likely as a consequence of loss of *de novo* ubiquitination mediated via RING1B.
314 Similarly, knockout of USP7 reduced H2AK119ub levels coinciding with reduced levels of RING1B
315 (Lecona et al., 2015). Other studies also show that USP7 is not likely a DUB for H2AK119 (Maertens et
316 al., 2010; Sarkari et al., 2009; van der Knaap et al., 2005). Thus, regulating ubiquitin levels within the
317 PRC1.1 complex itself is critically important and mediated via USP7 deubiquitinase activity.
318 With the efficient loss of PRC1.1 binding and consequent loss of H2AK119ub from target loci upon
319 USP7 inhibition we were able to study PRC1.1 function in relation to gene regulation in more detail.
320 Previously we identified genes that are targeted by PRC1.1 independent of H3K27me3 and have a
321 transcriptionally active profile suggested by H3K4me3, RNAPII and H3K27ac occupancy close to the
322 transcription start site. Loss of PRC1.1 binding resulted in reduced gene expression coinciding with
323 reduced levels of H3K27ac in the majority of analysed cases. The mechanisms underlying differences
324 in gene expression when PRC1.1 binding is lost are currently unclear. We hypothesize that PRC1.1
325 creates a transcriptionally permissive and open chromatin state which enables transcription factors
326 to bind and initiate gene expression. Addressing a possible cross-talk between PRC1.1 proteins,
327 CBP/p300-linked H3K27ac, recruitment of transcription factors and accessibility of chromatin is
328 definitely a focus for future work. Since H3K4me3 levels remained unaffected following USP7

329 inhibition, this suggest that the H3K4 methyltransferase complex that is likely targeted to CpGs via
330 CFP1 protein is not targeted in a PRC1.1-dependent manner (J. H. Lee & Skalnik, 2005).
331 In ESCs PRC1.1 targets are usually described together with canonical PRC1/PRC2 signaling, known as
332 bivalent loci and shown to repress target genes (Blackledge et al., 2014; Farcas et al., 2012; He et al.,
333 2013). For example, knockdown of KDM2B leads to the up-regulation of a subset of poised target
334 genes, coinciding with some reduction in RING1B binding and H2AK119ub (Farcas et al., 2012). While
335 we find no clear interaction of USP7 with canonical PRC1 in leukemic cells, it was shown that USP7
336 inhibition does impact functionally on canonical PRC1 (Lecona et al., 2015). Inhibiting the catalytic
337 core by removal of RING1A/B in ESCs does not lead to loss of KDM2B binding (Farcas et al., 2012).
338 However, in leukemic cells we find that USP7 inhibition not only leads to reduced H2AK119ub but
339 also induces loss of PRC1.1/KDM2B binding as a result of complex disassembly, suggesting that
340 KDM2B-PCGF1-BCOR/L1/SKP1 interactions might be needed for targeting. This is in agreement with
341 data that suggest that dimerization of PCGF1 and BCOR(L1) is required for binding to KDM2B and
342 recruiting PRC1.1 to the chromatin (Wong et al., 2016).
343 PRC1.1 is essential for human leukemic cells (van den Boom et al., 2016). By inhibiting individual
344 Polycomb proteins using an shRNA approach we observed impaired cell growth of leukemic cells
345 upon knockdown of PCGF1, RING1B, KDM2B or BCOR. *In vivo* experiments in humanized niche
346 xenograft mice using primary AML patient samples (Antonelli et al., 2016) or lentiviral leukemia
347 models (Sontakke et al., 2016) demonstrated that leukemogenesis was delayed or even abrogated
348 upon knockdown of PRC1.1 proteins. While these genetic studies clearly highlight the importance of
349 PRC1.1 for the survival of leukemic cells, small molecule inhibitors would be easier to implement in a
350 therapeutic clinical setting. Various USP7 inhibitors have been developed, and most recently
351 selective USP7 inhibitors which destabilize USP7 substrates including MDM2 and thereby increase
352 p53-mediated apoptosis of cancer cells were generated (Kategaya et al., 2017; Turnbull et al., 2017).
353 We observed that leukemic cells were very sensitive to USP7 inhibition, both in model systems as
354 well as in primary patient samples. Importantly, also the quiescent leukemic cells, that are usually

355 more difficult to target, showed sensitivity to P22077. It is evident that USP7 can function in several
356 pathways, often through regulating protein stability of tumor suppressors or epigenetic regulators
357 (Carra et al., 2017; Felle et al., 2011; van der Horst et al., 2006) and it is particularly the p53 pathway
358 that is strongly controlled by USP7 (Colland et al., 2009; Fan et al., 2013; M. Hu et al., 2006; Ye et al.,
359 2015). While we cannot exclude the possibility that some of these pathways were also affected in
360 some of our studies, we have analysed the p53 status in our models and primary AML patient
361 samples and see sensitivity even in the absence of a normal p53 response. Furthermore, while USP7
362 knockout mice are embryonically lethal, deletion of p53 was not able to rescue this phenotype,
363 further highlighting that p53-independent pathways downstream of USP7 exist as well (Kon et al.,
364 2010). Although P22077 has shown antitumor effects *in vivo* in neuroblastoma models (Fan et al.,
365 2013; Tavana et al., 2016), the responses that we observed *in vivo* in our CB MLL-AF9 leukemia model
366 were more modest, despite very strong effects seen upon USP7 inhibition *in vitro*. We wondered
367 whether the presence of a protective bone marrow microenvironment might play a role in regulating
368 P22077 sensitivity and therefore performed experiments in the absence or presence of bone marrow
369 stroma. We indeed demonstrate that MLL-AF9 cells grown on MS5 stromal cells were less sensitive
370 towards USP7 inhibition compared to cells grown in liquid culture conditions. These observations are
371 in line with other data clearly supporting the notion that the niche plays a protective role and can
372 dampen the response to therapeutic agents (Greim et al., 2014; Karjalainen et al., 2017; Parmar et
373 al., 2011).
374 In conclusion, our data reveal an important role for USP7 deubiquitinase activity in the integrity of
375 the PRC1.1 complex. We provide insight into the recruitment of PRC1.1 to target loci and function in
376 gene regulation and show that PRC1.1 is a potential interesting therapeutic target in leukemia.
377
378 **MATERIALS AND METHODS**
379 **GFP-mediated pull outs**

380 Pull outs were performed on nuclear extracts from K562 cells stably expressing KDM2B-EGFP, PCGF1-
381 EGFP and EGFP-RING1B. At least $80x10^6$ cells were collected for each pull out, washed with PBS and
382 lysed in 3 ml buffer A including freshly added protease inhibitors (10 mM HEPES/KOH pH 7.9, 1.5 mM
383 MgCl2, 10 mM KCl, 1 mM DTT, 1x Chymostatin Leupeptin Antipain Pepstatin (CLAP) protease-
384 inhibitor cocktail (all 1 µg/ml) and 0.1 mM PMSF (all from Sigma-Aldrich). After 10 minutes
385 incubation on ice, 10% IGEPAL CA-630 (endconc. 0.5%, Sigma-Aldrich) was added, followed by 10
386 seconds vortexing and 1 minute 14000 rpm spin to recover the nuclei. Nuclei were resuspended in
387 0.7 ml high salt buffer (20 mM HEPES/KOH pH 7.9, 1.5 mM MgCl2, 420 mM NaCl, 0.2 mM EDTA, 25%
388 Glycerol, 1 mM DTT, 1x CLAP and 0.1 mM PMSF) and incubated on ice for 20 minutes with 10
389 seconds vortexing intervals every 5 minutes. Extracted nuclei were collected after 15 minutes at
390 14000 rpm at 4°C and 2 volumes of Dilution buffer (25 mM Tris/Cl pH 7.5, 0.45% IGEPAL CA-630, 1 x
391 CLAP, 0.1 mM PMSF) and 3 volumes Wash buffer (TBS, 0.3% IGEPAL CA-630, 1 x CLAP, 0.1 mM PMSF)
392 were added. Pre-clearing of cell lysate was done by adding 50 µl pre-equilibrated binding control
393 magnetic agarose beads (Chromotek) and incubated for 30 min at 4°C on a rotating platform. Then
394 pre-cleared lysate was incubated with 70 µl pre-equilibrated GFP-Trap magnetic agarose beads
395 (Chromotek) overnight at 4°C on a rotating platform. Beads were separated using a magnetic rack
396 and six times washed in Wash buffer. Bound (B) fractions were eluted from the beads by boiling for
397 10 min in 2x Leammli sample buffer.
398
399 **In gel trypsin digestion**
400 Bound fractions of KDM2B-EGFP, PCGF1-EGFP (control/USP7i) and GFP-RING1B (control/USP7i) were
401 loaded on a 4-12% pre-cast NuPAGE gel (Invitrogen) and were run briefly. Gels were stained with
402 Coomassie dye R-250 (Thermo Scientific) and subsequently destained with ultrapure water
403 overnight. Gel lanes were cut into one slice, further cut into small pieces and completely destained
404 using 70% 50 mM $NH_4HCO_3$ and 30% acetonitrile (ACN). Reduction and alkylation of cysteines was
405 performed by adding 10 mM DTT dissolved in 50 mM $NH_4HCO_3$ and incubated at 55°C for 30 min.

406 Next, 55 mM iodoacetamide in 50 mM $NH_4HCO_3$ was added and incubated for 30 min, in dark, at
407 room temperature. Remaining fluid was removed and 50 mM $NH_4HCO_3$ was added with 10 min.
408 shaking. Then 100% ACN was added incubated for 30 min. while shaking. Fluid was removed and gel
409 pieces were dried for 15 min. at 55°C. Proteins were digested with adding 10 ng/µl sequencing-grade
410 modified trypsin (Promega) in 50 mM $NH_4HCO_3$ to the gel pieces and incubated overnight at 37°C.
411 Next day, peptides were extracted using 5% formic acid followed by second elution with 5% formic
412 acid in 75% acetonitrile. Samples were dried in a SpeedVac centrifuge and dissolved in 5% formic
413 acid.
414
415 **LC-MS/MS analysis**
416 Online chromatography of the extracted tryptic peptides was performed with the Ultimate 3000
417 nano-HPLC system (Thermo Fisher Scientific) coupled online to a Q-Exactive-Plus mass spectrometer
418 with a NanoFlex source (Thermo Fisher Scientific) equipped with a stainless steel emitter. Tryptic
419 digests were loaded onto a 5 mm × 300 µm i.d. trapping micro column packed with PepMAP100 5
420 µm particles (Dionex) in 0.1% FA at the flow rate of 20 µL/min. After loading and washing for 3
421 minutes, peptides were forward-flush eluted onto a 50 cm × 75 µm i.d. nanocolumn, packed with
422 Acclaim C18 PepMAP100 2 µm particles (Dionex). The following mobile phase gradient was delivered
423 at the flow rate of 300 nL/min: 2–50% of solvent B in 90 min; 50–80% B in 1 min; 80% B during 9 min,
424 and back to 2 % B in 1 min and held at 3% A for 19 minutes. Solvent A was 100:0 H2O/acetonitrile
425 (v/v) with 0.1% formic acid and solvent B was 0:100 H2O/acetonitrile (v/v) with 0.1% formic acid. MS
426 data were acquired using a data-dependent top-10 method dynamically choosing the most abundant
427 not-yet-sequenced precursor ions from the survey scans (300–1650 Th) with a dynamic exclusion of
428 20 seconds . Sequencing was performed via higher energy collisional dissociation fragmentation with
429 a target value of 2e5 ions determined with predictive automatic gain control. Isolation of precursors
430 was performed with a window of 1.6. Survey scans were acquired at a resolution of 70,000 at m/z
431 200. Resolution for HCD spectra was set to 17,500 at m/z 200 with a maximum ion injection time of

432 110 ms. The normalized collision energy was set at 28. Furthermore, the S-lens RF level was set at 60
433 and the capillary temperature was set at 250degr. C. Precursor ions with single, unassigned, or six
434 and higher charge states were excluded from fragmentation selection.

435 **Data analysis**

436 Raw mass spectrometry data were analysed using MaxQuant version 1.5.2.8 (Cox & Mann, 2008),
437 using default settings and LFQ/ iBAQ enabled, searched against the Human Uniprot/Swissprot
438 database (downloaded June 26, 2016, 20197 entries). Further data processing was performed using
439 Perseus software, version 1.5.6.0 (Tyanova et al., 2016). Network visualization of KDM2B interactome
440 was performed using Cytoscape software, version 3.5.1. For Gene Ontology (GO) analysis we used
441 DAVID Bioinformatics Resources (http://david.abcc.ncifcrf.gov/home.jsp). ChIP-seq tracks were
442 visualized and analysed using UCSC genome browser (http://genome.ucsc.edu). Accession number
443 for the Polycomb ChIP-seq data previously reported and used for analysis in this paper is GEO:
444 GSE54580 (van den Boom et al., 2016). Previously published ChIP-seq used for analysis include
445 H3K4me3, H3K36me3, H3K27ac and RNAPII/Pol2(b) from ENCODE/Broad Institute (GSE29611).

446

447 **Patient samples**

448 AML blasts from peripheral blood or bone marrow from untreated patients were studied after
449 informed consent and the protocol was approved by the Medical Ethical Committee, in accordance
450 with the Declaration of Helsinki. Mononuclear cells were isolated by density gradient centrifugation
451 and CD34+ cells were selected automatically by using autoMACS (Miltenyi Biotec).

452

453 **Cell culture**

454 The AML cell lines K562, MOLM13, NB4 and HL-60 were cultured in RPMI 1640 (BioWhittaker, Lonza,
455 Verviers, Belgium) supplemented with 10% fetal bovine serum (FCS, HyClone Laboratories, Logan,
456 Utah, US) and 1% penicillin/streptomycin (p/s, PAA Laboratories). KG1a cells were cultured in IMDM
457 (BioWhittaker), supplemented with 20% FCS and 1% p/s. MS5 murine stromal cells were cultured in

458 alpha-MEM with 200 mM glutamine (BioWhittaker) supplemented with 10% FCS and 1% p/s. Primary
459 AMLs were cultured in Gartner's medium consisting of alpha-MEM (BioWhittaker) supplemented
460 with 12.5% heat-inactivated FCS and 12.5% heat-inactivated Horse serum (Sigma-Aldrich, Saint Louis,
461 MO, USA), 1 µM hydrocortisone (Sigma-Aldrich), 57.2 µM β-mercaptoethanol (Sigma) and 1% p/s in
462 the presence of 20 ng/ml granulocyte colony-stimulating factor (G-CSF), thrombopoietin (TPO) and
463 IL-3. All AMLs were grown on a MS5 stromal layer. CB MLL-AF9 liquid and MS5 co-cultures under
464 myeloid permissive conditions were grown in Gartner's medium supplemented with 20 ng/ml Flt-3L,
465 stem cell factor (SCF) and IL-3 (Horton et al., 2013; Sontakke et al., 2016). For lymphoid CB-MLL-AF9
466 cells were grown on MS5 co-culture in Gartner's medium without Horse serum and hydrocortisone
467 and no IL-3 was added. Instead ascorbic acid (50 µg/ml, Sigma) and IL-7 (10 ng/ml) were added. All
468 cultures were kept at 37°C and 5% $CO_2$. For USP7 inhibition experiments, P22077 (1-(5-((2,4-
469 difluorophenyl)thio)-4-nitrothiophen-2-yl)ethanone) was purchased from Merck Millipore (662142)
470 (Billerica, MA, USA) and stock solution dissolved in DMSO then added 1:1000 to the culture.
471
472 **Generation of lentiviral vectors and transductions**
473 Lentiviral pRRL SFFV PCGF1-EGFP and EGFP-RING1B vectors were generated as described previously
474 (van den Boom, 2016). pRRL SFFV KDM2B EGFP was generated as follows. KDM2B was PCR amplified
475 from cDNA in two parts (from the ATG to the RsrII site [fragment 1] and from the RsrII site to end of
476 KDM2B [excluding the stop codon, fragment 2]). Both fragments were independently subcloned into
477 pJet1.2 resulting in the pJet1.2 KDM2B[1] and pJet1.2 KDM2B[2] plasmids and that were
478 subsequenty verified by sequencing. Next, KDM2B fragment 2 was isolated from pJet1.2 KDM2B[2]
479 using RsrII and XbaI digestion and ligated into pJet1.2 KDM2B[1] that was also digested with RsrII and
480 XbaI, resulting in a pJet1.2 plasmid with the full length KDM2B ORF but excluding the stop codon.
481 Finally, the KDM2B ORF was subcloned into the pRRL SFFV GFP vector using AgeI digestion, resulting
482 in the pRRL SFFV KDM2B-GFP construct. A lentiviral pRRL SFFV-His-Ubiquitin-mBlueberry2 vector was
483 generated by PCR amplification of His-Ubiquitin from pCl His-Ubi (Addgene) plasmid using primers

484 including BamHI sites. The PCR product was first ligated into pJet1.2 using Blunt-End cloning
485 protocol. Subsequently His-Ubiquitin was isolated from pJet1.2 using BamHI digestion and ligated
486 into pRRL SFFV-IRES-mBlueberry2 vector also using BamHI digestion and verified by sequencing.
487 Generation of lentiviral viruses and transductions were performed as described previously (van
488 Gosliga et al., 2007).
489
490 **Flow cytometry analysis**
491 Flow cytometry analyses were performed on the BD LSR II (Becton Dickinson (BD) Biosciences) and
492 data were analysed using FlowJo (Tree Star Inc, Ashland, OR, USA). Cells were sorted on a MoFlo XDP
493 or MoFLo Astrios (Beckman Coulter). For Hoechst/PyroninY staining, cells were resuspended in
494 HPGM (Lonza, Leusden, The Netherlands) and stained with 5 ug/ml Hoechst 33342 (Invitrogen) at
495 37°C for 30-45 min. Then 1 ug/ml PyroninY (Sigma) was added and incubated for 30-45 min at 37C.
496 Upon FcR blocking (MACS miltenyi Biotec), cells were stained with CD34-APC (581, BD Biosciences)
497 and CD38-AlexaFluor 700 (HIT2, Biolegend) at 4°C for 30 min. Cells were washed in medium
498 containing Hoechst/PyroninY and analysed on the BD LSR II. *In vivo* engraftment levels were analysed
499 in peripheral blood (PB), bone marrow, liver and spleen. Prior to staining, cells were blocked with
500 anti-human FcR block (MACS miltenyi Biotec) and anti-mouse CD16/CD32 block (BD Biosciences) and
501 stained with CD45-BV421 (HI30), CD19-BV785 (HIB19) and CD33-APC (WM53) all from Biolegend at
502 4°C for 30 min.
503
504 **Western blotting**
505 For detecting His-tagged ubiquitinated proteins cells were lysed in 1 ml denaturing lysis buffer (6M
506 Guanidium-HCl, 100 mM $Na_2HPO_4$ x $2H_2O$, 10 mM Tris-HCl pH 8.0, 5 mM Imidazole, 10 mM β-
507 mercaptoethanol) and sonicated on ice. Lysates were pre-cleared by centrifugation at 14000 rpm at
508 4°C and five volumes denaturing lysis buffer was added. His-tagged ubiquitinated proteins were
509 purified by adding 75 µl pre-equilibrated Ni-NTA magnetic agarose beads (Jena Bioscience) and

510 incubated for 4h on a rotating wheel. Beads were separated using a magnetic rack and washed 1x in
511 denaturing lysis buffer without Imidazole, 1x in wash buffer pH 8.0 (8M Urea, 100 mM $Na_2HPO_4$ x
512 $2H_2O$, 10 mM Tris-HCl pH 8.0 and 10 mM β-mercaptoethanol), 1x in wash buffer pH 6.3 (8M Urea,
513 100 mM $Na_2HPO_4$ x $2H_2O$, 10 mM Tris-HCl pH 6.3, 10 mM β-mercaptoethanol) plus 0.2% Triton X-100,
514 and 1x in wash buffer pH 6.3 plus 0.1% Triton X-100. His-tagged ubiquitinated proteins were eluted
515 from the beads by adding 75 µl elution buffer (200 mM Imidazole, 150 mM Tris-HCl pH 6.7, 30%
516 glycerol, 5% SDS and 720 mM β-mercaptoethanol) and incubated for 20 min. on a rotating wheel.
517 Elution samples were diluted 2x in Laemmli sample buffer containing 10% β-mercaptoethanol and
518 immediately boiled for 5 min. prior to Western blot analysis.
519 GFP mediated pull out cell lysates, input, non-bound and bound fractions were boiled for 5-10 min. in
520 Laemmli sample buffer prior to SDS-polyacrylamide gel electrophoresis. Proteins were transferred to
521 fluorescence polyvinylidene difluoride (PVDF FL, Millipore) membrane by semidry blotting.
522 Membranes were blocked in Odyssey blocking buffer (Westburg). The following primary antibodies
523 were used: anti-USP7 (A300-033A, Bethyl Laboratories), anti-RING1B (ab 181140, Abcam), anti-GFP
524 (sc-9996, Santa Cruz), anti-Ubiquitin (FK2, Enzo Life Sciences), anti-PCGF1 (ab183499, Abcam).
525 Fluorescent secondary antibodies either goat anti-mouse IRDye 800 or goat anti-rabbit IgG (H+L)
526 Alexa Fluor 680 (Invitrogen) were used for detection. Membranes were scanned using the Odyssey
527 CLx Imaging System (Li-Cor Biosciences).
528
529 **Chromatin immunoprecipitation**
530 ChIP was essentially performed as described previously (Frank, 2001), with minor modifications.
531 Briefly, K562 cells stably expressing low levels of EGFP-fusion vectors encoding, PCGF1-EGFP, EGFP-
532 RING1B, KDM2B-EGFP or non-transduced K562 cells and CB-MLL-AF9 cells were treated with DMSO
533 or P22077 for indicated timepoints and subsequently cross-linked with 1% formaldehyde for 10 min.
534 Reactions were quenched with addition of Glycine at a final concentration of 125 mM. Cells were
535 lysed in SDS buffer including protease inhibitors (1x CLAP, 0.1 mM PMSF) and snap frozen in liquid

536 nitrogen and stored at -80°C. ChIP was continued by resuspending cells in cold IP buffer and
537 sonicated using a Bioruptor (Diagenode). Pre-clearing was performed by adding Protein G Dynabeads
538 (Invitrogen) and incubated for 15 min at 4°C on a rotating platform. Then ChIP reactions were
539 performed using the following antibodies: anti-GFP (ab290, Abcam), anti-KDM2B (ab137547, Abcam),
540 anti-H2AK119ub (D27C4, Cell Signaling Technology), anti-H3K4me3 (ab8580, Abcam), anti-H3K27ac
541 (C15410196, Diagenode) and IgG (I8141, Sigma) followed by overnight incubation at 4°C on a rotating
542 platform. Next day Protein G Dynabeads were added for 2-4h after beads were separated using a
543 magnetic rack and washed with 3x Mixed Micelle Buffer, 2x Buffer 500, 2x LiCl Detergent Wash
544 Buffer and 1x TE (pH 8.0). ChIP DNA was eluted and reverse cross-linked at 65°C in the presence of
545 1% SDS and 0.1M $NaHCO_3$. Samples were treated with RNase and Proteinase K and purified using
546 QIAquick PCR purification kit (Qiagen). ChIPs were analysed by qPCR as percentage of input, primer
547 sequences are available on request.
548
549 **RNA seq analysis and quantitative real-time PCR**
550 RNA samples for sequencing were prepared for DMSO and P22077 (30 μM) treated K562 cells at 4h,
551 8h, 16h and 24h. Total RNA was isolated using the RNeasy Mini Kit from Qiagen (Venlo, The
552 Netherlands) according to the manufacturer's recommendations. Initial quality check and RNA
553 quantification of the samples was performed by capillary electrophoresis using the LabChip GX
554 (Perkin Elmer). Sequence libraries were generated with 50 ng mRNA, using Lexogen Quantseq 3' prep
555 kit (Lexogen GmbH) according to the manufacturer's recommendations. The obtained cDNA
556 fragment libraries were sequenced on an Illumina NextSeq500 using default parameters (single
557 read). Bioinformatics were performed on the Strand Avadis NGS (v3.0) software (Strand Life Sciences
558 Pvt.Ltd). Sequence quality was checked for GC content, base quality and composition using FASTQC
559 and StrandNGS. Quality trimmed reads were aligned to build Human Hg19 transcriptome. Ensembl
560 Genes and transcripts (2014.01.02) was used as gene annotation database. Quantified reads were

561 normalized using the DESeq package. Reads with failed vendor QC, quality score less than 24
562 (average), mapping quality score below 50 and length less than 20 were all filtered out.
563 For quantitative RT-PCR, RNA was reverse transcribed using the iScript cDNA synthesis kit (Bio-Rad)
564 and amplified using SsoAdvanced SYBR Green Supermix (Bio-Rad) on a CFX384 Touch Real-Time PCR
565 Detection System (Bio-Rad). RPL27 was used as housekeeping gene. Primer sequences are available
566 on request.
567
568 **USP7 inhibition *in vivo***
569 Eight to ten week old female NSG (NOD.Cg-Prkdcscid Il2rgtm1Wjl/SzJ) mice were purchased from the
570 Centrale Dienst Proefdieren (CDP) breeding facility within the University Medical Center Groningen.
571 Mouse experiments were performed in accordance with national and institutional guidelines, and all
572 experiments were approved by the Institutional Animal Care and Use Committee of the University of
573 Groningen (IACUC-RuG). 24h prior to transplantations, mice were sub-lethally irradiated with a dose
574 of 1.0 Gy (X-RAD 320 Unit, PXINC 2010). After irradiation mice received Neomycin (3.5 g/l) in their
575 drinking water and soft food (RM Convalescence + BG SY (M); Special Diet Services; Witham,
576 England) for two weeks. For secondary transplantations, 5 x $10^4$ MLL-AF9 EGFP cells from primary
577 leukemic mice (CB MLL-AF9 xenograft mouse model, (Horton et al., 2013; Sontakke et al., 2016))
578 were injected IV (lateral tail vein). Peripheral blood chimerism levels were monitored by regular
579 blood sample analysis. Mice were randomly divided into two groups, weighted and treated with
580 DMSO as control (n=5) or 20 mg/kg P22077 (n=6) via intraperitoneal (IP) injections daily starting four
581 weeks post-transplant. Prior to injections, P22077 was dissolved in DMSO (or DMSO only as control)
582 and directly mixed with Cremophor EL (1:1). This solution was then diluted 1:4 in saline, to get an end
583 concentration of max. 10% DMSO. Mice were humanely terminated by cervical dislocation under
584 isoflurane anesthesia when chimerism levels in the blood exceeded 40%. Peripheral blood, bone
585 marrow, spleen and liver were analysed.
586

587 **Acknowledgments**

588 The authors thank Dr. S. Bergink and E. de Mattos for providing pCl His-Ubi plasmid and advice with
589 ubiquitin experiments. We thank M. Elliot for generation of KDM2B-EGFP construct. We would like to
590 thank Roelof-Jan van der Lei, Theo Bijma, Henk Moes en Geert Mesander for help with cell sorting.
591 We acknowledge Prof. Robert E Campbell (Department of Chemistry, University of Alberta,
592 Edmonton, Alberta, Canada) for providing the mBlueberry2 Fluorescent Protein. This work is
593 supported by the European Research Council (ERC-2011-StG 281474-huLSCtargeting) and the Dutch
594 Cancer Foundation (RUG 2014-6832).

595

596 **Competing interest**

597 The authors declare no competing interests.

Reference List


Altun, M., Kramer, H. B., Willems, L. I., McDermott, J. L., Leach, C. A., Goldenberg, S. J., . . . Kessler, B. M. (2011). Activity-based chemical proteomics accelerates inhibitor development for deubiquitylating enzymes. *Chem Biol, 18*(11), 1401-1412. doi:10.1016/j.chembiol.2011.08.018

Andricovich, J., Kai, Y., Peng, W., Foudi, A., & Tzatsos, A. (2016). Histone demethylase KDM2B regulates lineage commitment in normal and malignant hematopoiesis. *J. Clin. Invest*. doi:84014 [pii];10.1172/JCI84014 [doi]

Antonelli, A., Noort, W. A., Jaques, J., de, B. B., de Jong-Korlaar, R., Brouwers-Vos, A. Z., . . . Schuringa, J. J. (2016). Establishing human leukemia xenograft mouse models by implanting human bone marrow-like scaffold-based niches. *Blood, 128*(25), 2949-2959. doi:blood-2016-05-719021 [pii];10.1182/blood-2016-05-719021 [doi]

Ben-Saadon, R., Zaaroor, D., Ziv, T., & Ciechanover, A. (2006). The polycomb protein Ring1B generates self atypical mixed ubiquitin chains required for its in vitro histone H2A ligase activity. *Mol Cell, 24*(5), 701-711. doi:10.1016/j.molcel.2006.10.022

Blackledge, N. P., Farcas, A. M., Kondo, T., King, H. W., McGouran, J. F., Hanssen, L. L., . . . Klose, R. J. (2014). Variant PRC1 complex-dependent H2A ubiquitylation drives PRC2 recruitment and polycomb domain formation. *Cell, 157*(6), 1445-1459. doi:S0092-8674(14)00589-3 [pii];10.1016/j.cell.2014.05.004 [doi]

Boulard, M., Edwards, J. R., & Bestor, T. H. (2015). FBXL10 protects Polycomb-bound genes from hypermethylation. *Nat. Genet, 47*(5), 479-485. doi:ng.3272 [pii];10.1038/ng.3272 [doi]

Boyer, L. A., Plath, K., Zeitlinger, J., Brambrink, T., Medeiros, L. A., Lee, T. I., . . . Jaenisch, R. (2006). Polycomb complexes repress developmental regulators in murine embryonic stem cells. *Nature, 441*(7091), 349-353.

Bracken, A. P., Dietrich, N., Pasini, D., Hansen, K. H., & Helin, K. (2006). Genome-wide mapping of Polycomb target genes unravels their roles in cell fate transitions. *Genes Dev, 20*(9), 1123-1136.

Bracken, A. P., & Helin, K. (2009). Polycomb group proteins: navigators of lineage pathways led astray in cancer. *Nat. Rev. Cancer, 9*(11), 773-784. doi:nrc2736 [pii];10.1038/nrc2736 [doi]

Buchwald, G., van der Stoop, P., Weichenrieder, O., Perrakis, A., van, L. M., & Sixma, T. K. (2006). Structure and E3-ligase activity of the Ring-Ring complex of polycomb proteins Bmi1 and Ring1b. *EMBO J, 25*(11), 2465-2474. doi:7601144 [pii];10.1038/sj.emboj.7601144 [doi]

Cao, R., Tsukada, Y., & Zhang, Y. (2005). Role of Bmi-1 and Ring1A in H2A ubiquitylation and Hox gene silencing. *Mol. Cell, 20*(6), 845-854. doi:S1097-2765(05)01817-4 [pii];10.1016/j.molcel.2005.12.002 [doi]

Cao, R., Wang, L., Wang, H., Xia, L., Erdjument-Bromage, H., Tempst, P., . . . Zhang, Y. (2002). Role of histone H3 lysine 27 methylation in Polycomb-group silencing. *Science, 298*(5595), 1039-1043.

Carra, G., Panuzzo, C., Torti, D., Parvis, G., Crivellaro, S., Familiari, U., . . . Morotti, A. (2017). Therapeutic inhibition of USP7-PTEN network in chronic lymphocytic leukemia: a strategy to overcome TP53 mutated/deleted clones. *Oncotarget, 8*(22), 35508-35522. doi:10.18632/oncotarget.16348

Colland, F., Formstecher, E., Jacq, X., Reverdy, C., Planquette, C., Conrath, S., . . . Daviet, L. (2009). Small-molecule inhibitor of USP7/HAUSP ubiquitin protease stabilizes and activates p53 in cells. *Mol Cancer Ther, 8*(8), 2286-2295. doi:10.1158/1535-7163.MCT-09-0097

Cox, J., & Mann, M. (2008). MaxQuant enables high peptide identification rates, individualized p.p.b.-range mass accuracies and proteome-wide protein quantification. *Nat. Biotechnol, 26*(12), 1367-1372. doi:nbt.1511 [pii];10.1038/nbt.1511 [doi]

de, B. P., Zaaroor-Regev, D., & Ciechanover, A. (2010). Regulation of the Polycomb protein RING1B ubiquitination by USP7. *Biochem. Biophys. Res. Commun, 400*(3), 389-395. doi:S0006-291X(10)01592-5 [pii];10.1016/j.bbrc.2010.08.082 [doi]

de Napoles, M., Mermoud, J. E., Wakao, R., Tang, Y. A., Endoh, M., Appanah, R., . . . Brockdorff, N. (2004). Polycomb group proteins Ring1A/B link ubiquitylation of histone H2A to heritable gene silencing and X inactivation. *Dev. Cell, 7*(5), 663-676.

Dou, H., Buetow, L., Sibbet, G. J., Cameron, K., & Huang, D. T. (2012). BIRC7-E2 ubiquitin conjugate structure reveals the mechanism of ubiquitin transfer by a RING dimer. *Nat Struct Mol Biol, 19*(9), 876-883. doi:10.1038/nsmb.2379

Elderkin, S., Maertens, G. N., Endoh, M., Mallery, D. L., Morrice, N., Koseki, H., . . . Hiom, K. (2007). A phosphorylated form of Mel-18 targets the Ring1B histone H2A ubiquitin ligase to chromatin. *Mol. Cell, 28*(1), 107-120. doi:S1097-2765(07)00552-7 [pii];10.1016/j.molcel.2007.08.009 [doi]

Endoh, M., Endo, T. A., Endoh, T., Fujimura, Y., Ohara, O., Toyoda, T., . . . Koseki, H. (2008). Polycomb group proteins Ring1A/B are functionally linked to the core transcriptional regulatory circuitry to maintain ES cell identity. *Development, 135*(8), 1513-1524. doi:10.1242/dev.014340

Engelen, E., Brandsma, J. H., Moen, M. J., Signorile, L., Dekkers, D. H., Demmers, J., . . . Poot, R. A. (2015). Proteins that bind regulatory regions identified by histone modification chromatin immunoprecipitations and mass spectrometry. *Nat. Commun, 6*, 7155. doi:ncomms8155 [pii];10.1038/ncomms8155 [doi]

Fan, Y. H., Cheng, J., Vasudevan, S. A., Dou, J., Zhang, H., Patel, R. H., . . . Yang, J. (2013). USP7 inhibitor P22077 inhibits neuroblastoma growth via inducing p53-mediated apoptosis. *Cell Death Dis, 4*, e867. doi:10.1038/cddis.2013.400

Farcas, A. M., Blackledge, N. P., Sudbery, I., Long, H. K., McGouran, J. F., Rose, N. R., . . . Klose, R. J. (2012). KDM2B links the Polycomb Repressive Complex 1 (PRC1) to recognition of CpG islands. *Elife, 1*, e00205. doi:10.7554/eLife.00205 [doi];00205 [pii]

Felle, M., Joppien, S., Nemeth, A., Diermeier, S., Thalhammer, V., Dobner, T., . . . Langst, G. (2011). The USP7/Dnmt1 complex stimulates the DNA methylation activity of Dnmt1 and regulates the stability of UHRF1. *Nucleic Acids Res, 39*(19), 8355-8365. doi:10.1093/nar/gkr528

Francis, N. J., Kingston, R. E., & Woodcock, C. L. (2004). Chromatin compaction by a polycomb group protein complex. *Science, 306*(5701), 1574-1577. doi:10.1126/science.1100576

Gao, Z., Zhang, J., Bonasio, R., Strino, F., Sawai, A., Parisi, F., . . . Reinberg, D. (2012). PCGF Homologs, CBX Proteins, and RYBP Define Functionally Distinct PRC1 Family Complexes. *Mol. Cell, 45*(3), 344-356. doi:S1097-2765(12)00035-4 [pii];10.1016/j.molcel.2012.01.002 [doi]

Gearhart, M. D., Corcoran, C. M., Wamstad, J. A., & Bardwell, V. J. (2006). Polycomb group and SCF ubiquitin ligases are found in a novel BCOR complex that is recruited to BCL6 targets. *Mol. Cell Biol, 26*(18), 6880-6889. doi:26/18/6880 [pii];10.1128/MCB.00630-06 [doi]

Greim, H., Kaden, D. A., Larson, R. A., Palermo, C. M., Rice, J. M., Ross, D., & Snyder, R. (2014). The bone marrow niche, stem cells, and leukemia: impact of drugs, chemicals, and the environment. *Ann. N. Y. Acad. Sci, 1310*, 7-31. doi:10.1111/nyas.12362 [doi]

He, J., Nguyen, A. T., & Zhang, Y. (2011). KDM2b/JHDM1b, an H3K36me2-specific demethylase, is required for initiation and maintenance of acute myeloid leukemia. *Blood, 117*(14), 3869-3880. doi:blood-2010-10-312736 [pii];10.1182/blood-2010-10-312736 [doi]

He, J., Shen, L., Wan, M., Taranova, O., Wu, H., & Zhang, Y. (2013). Kdm2b maintains murine embryonic stem cell status by recruiting PRC1 complex to CpG islands of developmental genes. *Nat. Cell Biol, 15*(4), 373-384. doi:ncb2702 [pii];10.1038/ncb2702 [doi]

Horton, S. J., Jaques, J., Woolthuis, C., van, D. J., Mesuraca, M., Huls, G., . . . Schuringa, J. J. (2013). MLL-AF9-mediated immortalization of human hematopoietic cells along different lineages changes during ontogeny. *Leukemia, 27*(5), 1116-1126. doi:leu2012343 [pii];10.1038/leu.2012.343 [doi]

Hu, D., & Shilatifard, A. (2016). Epigenetics of hematopoiesis and hematological malignancies. *Genes Dev, 30*(18), 2021-2041. doi:30/18/2021 [pii];10.1101/gad.284109.116 [doi]

Hu, M., Gu, L., Li, M., Jeffrey, P. D., Gu, W., & Shi, Y. (2006). Structural basis of competitive recognition of p53 and MDM2 by HAUSP/USP7: implications for the regulation of the p53-MDM2 pathway. *PLoS Biol, 4*(2), e27. doi:10.1371/journal.pbio.0040027

Junco, S. E., Wang, R., Gaipa, J. C., Taylor, A. B., Schirf, V., Gearhart, M. D., . . . Kim, C. A. (2013). Structure of the Polycomb Group Protein PCGF1 in Complex with BCOR Reveals Basis for Binding Selectivity of PCGF Homologs. *Structure*. doi:S0969-2126(13)00053-1 [pii];10.1016/j.str.2013.02.013 [doi]

Karjalainen, R., Pemovska, T., Popa, M., Liu, M., Javarappa, K. K., Majumder, M. M., . . . Heckman, C. A. (2017). JAK1/2 and BCL2 inhibitors synergize to counteract bone marrow stromal cell-induced protection of AML. *Blood, 130*(6), 789-802. doi:10.1182/blood-2016-02-699363

Kategaya, L., Di Lello, P., Rouge, L., Pastor, R., Clark, K. R., Drummond, J., . . . Wertz, I. E. (2017). USP7 small-molecule inhibitors interfere with ubiquitin binding. *Nature*. doi:10.1038/nature24006

Kirmizis, A., Bartley, S. M., Kuzmichev, A., Margueron, R., Reinberg, D., Green, R., & Farnham, P. J. (2004). Silencing of human polycomb target genes is associated with methylation of histone H3 Lys 27. *Genes Dev, 18*(13), 1592-1605. doi:10.1101/gad.1200204

Kon, N., Kobayashi, Y., Li, M., Brooks, C. L., Ludwig, T., & Gu, W. (2010). Inactivation of HAUSP in vivo modulates p53 function. *Oncogene, 29*(9), 1270-1279. doi:10.1038/onc.2009.427

Kottakis, F., Foltopoulou, P., Sanidas, I., Keller, P., Wronski, A., Dake, B. T., . . . Tsichlis, P. N. (2014). NDY1/KDM2B Functions as a Master Regulator of Polycomb Complexes and Controls Self-Renewal of Breast Cancer Stem Cells. *Cancer Res, 74*(14), 3935-3946. doi:0008-5472.CAN-13-2733 [pii];10.1158/0008-5472.CAN-13-2733 [doi]

Kouzarides, T. (2007). Chromatin modifications and their function. *Cell, 128*(4), 693-705. doi:S0092-8674(07)00184-5 [pii];10.1016/j.cell.2007.02.005 [doi]

Kuzmichev, A., Nishioka, K., Erdjument-Bromage, H., Tempst, P., & Reinberg, D. (2002). Histone methyltransferase activity associated with a human multiprotein complex containing the Enhancer of Zeste protein. *Genes Dev, 16*(22), 2893-2905.

Lecona, E., Narendra, V., & Reinberg, D. (2015). USP7 COOPERATES WITH SCML2 TO REGULATE THE ACTIVITY OF PRC1. *Mol. Cell Biol*. doi:MCB.01197-14 [pii];10.1128/MCB.01197-14 [doi]

Lee, J. H., & Skalnik, D. G. (2005). CpG-binding protein (CXXC finger protein 1) is a component of the mammalian Set1 histone H3-Lys4 methyltransferase complex, the analogue of the yeast Set1/COMPASS complex. *J Biol Chem, 280*(50), 41725-41731. doi:10.1074/jbc.M508312200

Lee, T. I., Jenner, R. G., Boyer, L. A., Guenther, M. G., Levine, S. S., Kumar, R. M., . . . Young, R. A. (2006). Control of developmental regulators by Polycomb in human embryonic stem cells. *Cell, 125*(2), 301-313. doi:10.1016/j.cell.2006.02.043

Leznicki, P., & Kulathu, Y. (2017). Mechanisms of regulation and diversification of deubiquitylating enzyme function. *J Cell Sci, 130*(12), 1997-2006. doi:10.1242/jcs.201855

Li, M., Brooks, C. L., Kon, N., & Gu, W. (2004). A dynamic role of HAUSP in the p53-Mdm2 pathway. *Mol Cell, 13*(6), 879-886.

Liang, G., He, J., & Zhang, Y. (2012). Kdm2b promotes induced pluripotent stem cell generation by facilitating gene activation early in reprogramming. *Nat. Cell Biol, 14*(5), 457-466. doi:ncb2483 [pii];10.1038/ncb2483 [doi]

Maertens, G. N., El Messaoudi-Aubert, S., Elderkin, S., Hiom, K., & Peters, G. (2010). Ubiquitin-specific proteases 7 and 11 modulate Polycomb regulation of the INK4a tumour suppressor. *EMBO J, 29*(15), 2553-2565. doi:10.1038/emboj.2010.129

Mas, G., & Di, C. L. (2016). The role of Polycomb in stem cell genome architecture. *Curr. Opin. Cell Biol, 43*, 87-95. doi:S0955-0674(16)30155-7 [pii];10.1016/j.ceb.2016.09.006 [doi]

Morey, L., Santanach, A., Blanco, E., Aloia, L., Nora, E. P., Bruneau, B. G., & Di, C. L. (2015). Polycomb Regulates Mesoderm Cell Fate-Specification in Embryonic Stem Cells through Activation and Repression Mechanisms. *Cell Stem Cell, 17*(3), 300-315. doi:S1934-5909(15)00364-1 [pii];10.1016/j.stem.2015.08.009 [doi]

750 Muller, J., & Verrijzer, P. (2009). Biochemical mechanisms of gene regulation by polycomb group
751 protein complexes. *Curr Opin Genet Dev, 19*(2), 150-158. doi:10.1016/j.gde.2009.03.001
752 Ning, B., Zhao, W., Qian, C., Liu, P., Li, Q., Li, W., & Wang, R. F. (2017). USP26 functions as a negative
753 regulator of cellular reprogramming by stabilising PRC1 complex components. *Nat. Commun,*
754 *8*(1), 349. doi:10.1038/s41467-017-00301-4 [doi];10.1038/s41467-017-00301-4 [pii]
755 Parmar, A., Marz, S., Rushton, S., Holzwarth, C., Lind, K., Kayser, S., . . . Gotze, K. S. (2011). Stromal
756 niche cells protect early leukemic FLT3-ITD+ progenitor cells against first-generation FLT3
757 tyrosine kinase inhibitors. *Cancer Res, 71*(13), 4696-4706. doi:10.1158/0008-5472.CAN-10-
758 4136
759 Piunti, A., & Shilatifard, A. (2016). Epigenetic balance of gene expression by Polycomb and COMPASS
760 families. *Science, 352*(6290), aad9780. doi:10.1126/science.aad9780
761 Rose, N. R., King, H. W., Blackledge, N. P., Fursova, N. A., Ember, K. J., Fischer, R., . . . Klose, R. J.
762 (2016). RYBP stimulates PRC1 to shape chromatin-based communication between Polycomb
763 repressive complexes. *Elife, 5*. doi:10.7554/eLife.18591 [doi]
764 Sanchez, C., Sanchez, I., Demmers, J. A., Rodriguez, P., Strouboulis, J., & Vidal, M. (2007). Proteomics
765 analysis of Ring1B/Rnf2 interactors identifies a novel complex with the Fbxl10/Jhdm1B
766 histone demethylase and the Bcl6 interacting corepressor. *Mol. Cell Proteomics, 6*(5), 820-
767 834. doi:M600275-MCP200 [pii];10.1074/mcp.M600275-MCP200 [doi]
768 Sarkari, F., Sanchez-Alcaraz, T., Wang, S., Holowaty, M. N., Sheng, Y., & Frappier, L. (2009). EBNA1-
769 mediated recruitment of a histone H2B deubiquitylating complex to the Epstein-Barr virus
770 latent origin of DNA replication. *PLoS Pathog, 5*(10), e1000624.
771 doi:10.1371/journal.ppat.1000624
772 Simon, J. A., & Kingston, R. E. (2009). Mechanisms of polycomb gene silencing: knowns and
773 unknowns. *Nat. Rev. Mol. Cell Biol, 10*(10), 697-708. doi:nrm2763 [pii];10.1038/nrm2763
774 [doi]
775 Simon, J. A., & Kingston, R. E. (2013). Occupying chromatin: Polycomb mechanisms for getting to
776 genomic targets, stopping transcriptional traffic, and staying put. *Mol. Cell, 49*(5), 808-824.
777 doi:S1097-2765(13)00141-X [pii];10.1016/j.molcel.2013.02.013 [doi]
778 Sontakke, P., Carretta, M., Jaques, J., Brouwers-Vos, A. Z., Lubbers-Aalders, L., Yuan, H., . . .
779 Schuringa, J. J. (2016). Modeling BCR-ABL and MLL-AF9 leukemia in a human bone marrow-
780 like scaffold-based xenograft model. *Leukemia, 30*(10), 2064-2073. doi:leu2016108
781 [pii];10.1038/leu.2016.108 [doi]
782 Taherbhoy, A. M., Huang, O. W., & Cochran, A. G. (2015). BMI1-RING1B is an autoinhibited RING E3
783 ubiquitin ligase. *Nat. Commun, 6*, 7621. doi:ncomms8621 [pii];10.1038/ncomms8621 [doi]
784 Tavana, O., Li, D., Dai, C., Lopez, G., Banerjee, D., Kon, N., . . . Gu, W. (2016). HAUSP deubiquitinates
785 and stabilizes N-Myc in neuroblastoma. *Nat Med, 22*(10), 1180-1186. doi:10.1038/nm.4180
786 Tavares, Λ., Dimitrova, E., Oxley, D., Webster, J., Poot, R., Demmers, J., . . . Brockdorff, N. (2012).
787 RYBP-PRC1 Complexes Mediate H2A Ubiquitylation at Polycomb Target Sites Independently
788 of PRC2 and H3K27me3. *Cell*.
789 Tian, X., Isamiddinova, N. S., Peroutka, R. J., Goldenberg, S. J., Mattern, M. R., Nicholson, B., & Leach,
790 C. (2011). Characterization of selective ubiquitin and ubiquitin-like protease inhibitors using a
791 fluorescence-based multiplex assay format. *Assay Drug Dev Technol, 9*(2), 165-173.
792 doi:10.1089/adt.2010.0317
793 Turnbull, A. P., Ioannidis, S., Krajewski, W. W., Pinto-Fernandez, A., Heride, C., Martin, A. C. L., . . .
794 Komander, D. (2017). Molecular basis of USP7 inhibition by selective small-molecule
795 inhibitors. *Nature*. doi:10.1038/nature24451
796 Tyanova, S., Temu, T., Sinitcyn, P., Carlson, A., Hein, M. Y., Geiger, T., . . . Cox, J. (2016). The Perseus
797 computational platform for comprehensive analysis of (prote)omics data. *Nat. Methods,*
798 *13*(9), 731-740. doi:nmeth.3901 [pii];10.1038/nmeth.3901 [doi]
799 Tzatsos, A., Pfau, R., Kampranis, S. C., & Tsichlis, P. N. (2009). Ndy1/KDM2B immortalizes mouse
800 embryonic fibroblasts by repressing the Ink4a/Arf locus. *Proc. Natl. Acad. Sci. U. S. A, 106*(8),
801 2641-2646. doi:0813139106 [pii];10.1073/pnas.0813139106 [doi]

802 Ueda, T., Nagamachi, A., Takubo, K., Yamasaki, N., Matsui, H., Kanai, A., . . . Honda, H. (2015). Fbxl10
803 overexpression in murine hematopoietic stem cells induces leukemia involving metabolic
804 activation and upregulation of Nsg2. *Blood*. doi:blood-2014-03-562694 [pii];10.1182/blood-
805 2014-03-562694 [doi]
806 van den Boom, V., Maat, H., Geugien, M., Rodriguez, L. A., Sotoca, A. M., Jaques, J., . . . Schuringa, J. J.
807 (2016). Non-canonical PRC1.1 Targets Active Genes Independent of H3K27me3 and Is
808 Essential for Leukemogenesis. *Cell Rep, 14*(2), 332-346. doi:S2211-1247(15)01458-8
809 [pii];10.1016/j.celrep.2015.12.034 [doi]
810 van den Boom, V., Rozenveld-Geugien, M., Bonardi, F., Malanga, D., van, G. D., Heijink, A. M., . . .
811 Schuringa, J. J. (2013). Non-redundant and locus-specific gene repression functions of PRC1
812 paralog family members in human hematopoietic stem/progenitor cells. *Blood, 121*(13),
813 2452-2461. doi:blood-2012-08-451666 [pii];10.1182/blood-2012-08-451666 [doi]
814 van der Horst, A., de Vries-Smits, A. M., Brenkman, A. B., van Triest, M. H., van den Broek, N.,
815 Colland, F., . . . Burgering, B. M. (2006). FOXO4 transcriptional activity is regulated by
816 monoubiquitination and USP7/HAUSP. *Nat Cell Biol, 8*(10), 1064-1073. doi:10.1038/ncb1469
817 van der Knaap, J. A., Kumar, B. R., Moshkin, Y. M., Langenberg, K., Krijgsveld, J., Heck, A. J., . . .
818 Verrijzer, C. P. (2005). GMP synthetase stimulates histone H2B deubiquitylation by the
819 epigenetic silencer USP7. *Mol Cell, 17*(5), 695-707. doi:10.1016/j.molcel.2005.02.013
820 van Gosliga, D., Schepers, H., Rizo, A., van der Kolk, D., Vellenga, E., & Schuringa, J. J. (2007).
821 Establishing long-term cultures with self-renewing acute myeloid leukemia stem/progenitor
822 cells. *Exp. Hematol, 35*(10), 1538-1549.
823 Wang, H., Wang, L., Erdjument-Bromage, H., Vidal, M., Tempst, P., Jones, R. S., & Zhang, Y. (2004).
824 Role of histone H2A ubiquitination in Polycomb silencing. *Nature, 431*(7010), 873-878.
825 doi:10.1038/nature02985 [doi];nature02985 [pii]
826 Wang, R., Taylor, A. B., Leal, B. Z., Chadwell, L. V., Ilangovan, U., Robinson, A. K., . . . Kim, C. A. (2010).
827 Polycomb group targeting through different binding partners of RING1B C-terminal domain.
828 *Structure, 18*(8), 966-975. doi:S0969-2126(10)00220-0 [pii];10.1016/j.str.2010.04.013 [doi]
829 Wong, S. J., Gearhart, M. D., Taylor, A. B., Nanyes, D. R., Ha, D. J., Robinson, A. K., . . . Kim, C. A.
830 (2016). KDM2B Recruitment of the Polycomb Group Complex, PRC1.1, Requires Cooperation
831 between PCGF1 and BCORL1. *Structure*. doi:S0969-2126(16)30222-2
832 [pii];10.1016/j.str.2016.07.011 [doi]
833 Wu, X., Johansen, J. V., & Helin, K. (2013). Fbxl10/Kdm2b Recruits Polycomb Repressive Complex 1 to
834 CpG Islands and Regulates H2A Ubiquitylation. *Mol. Cell, 49*(6), 1134-1146. doi:S1097-
835 2765(13)00049-X [pii];10.1016/j.molcel.2013.01.016 [doi]
836 Ye, M., Tang, Y., Tang, S., Liu, J., Wu, K., Yao, S., . . . Tan, W. (2015). STIP is a critical nuclear
837 scaffolding protein linking USP7 to p53-Mdm2 pathway regulation. *Oncotarget, 6*(33), 34718-
838 34731. doi:10.18632/oncotarget.5303

839

840

841

842 **Figures and Figure legends**

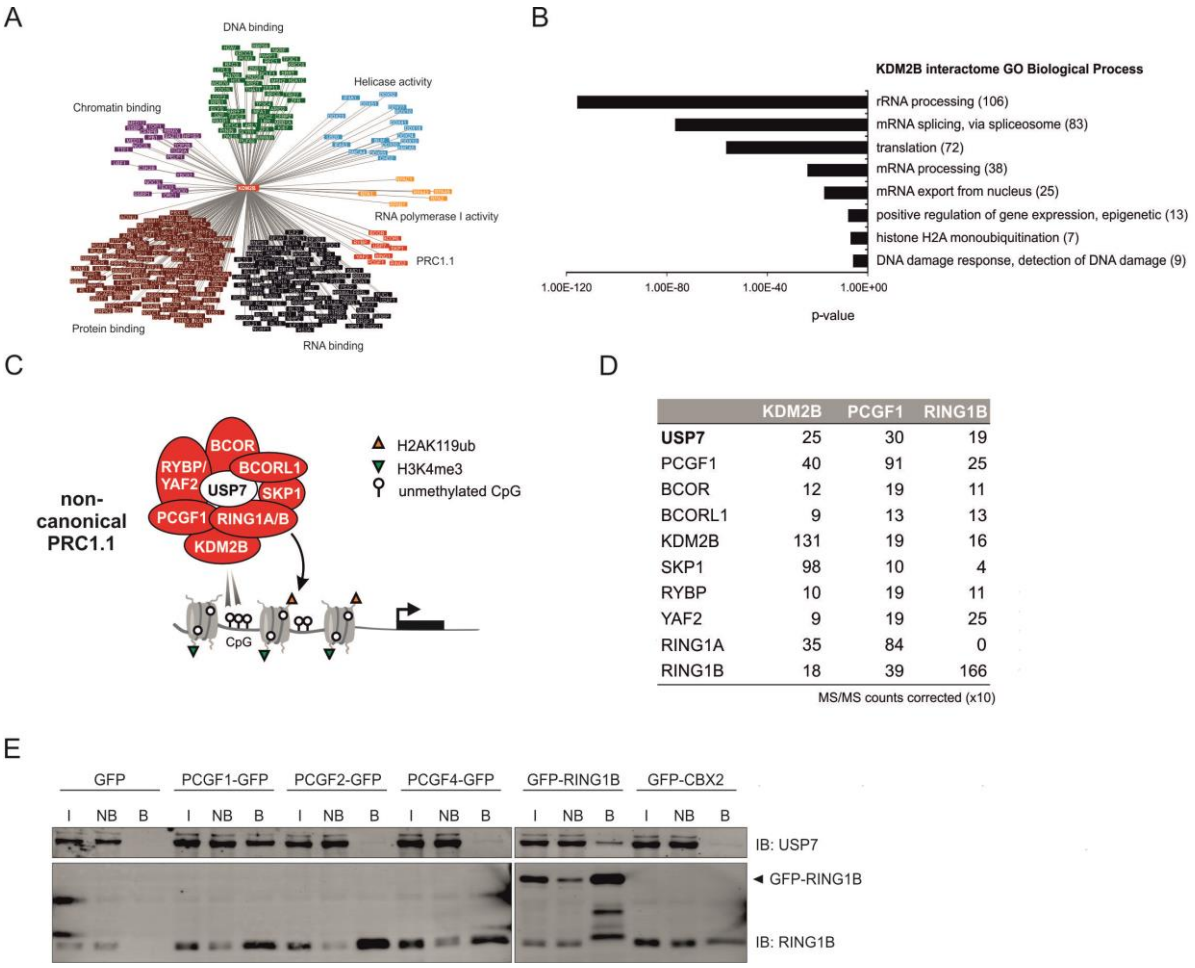


| | KDM2B | PCGF1 | RING1B |
|---|---|---|---|
| **USP7** | 25 | 30 | 19 |
| PCGF1 | 40 | 91 | 25 |
| BCOR | 12 | 19 | 11 |
| BCORL1 | 9 | 13 | 13 |
| KDM2B | 131 | 19 | 16 |
| SKP1 | 98 | 10 | 4 |
| RYBP | 10 | 19 | 11 |
| YAF2 | 9 | 19 | 25 |
| RING1A | 35 | 84 | 0 |
| RING1B | 18 | 39 | 166 |

MS/MS counts corrected (x10)

843

844

845 **Figure 1. The deubiquitinase USP7 interacts with non-canonical PRC1.1 proteins**

846 (A) Visualization of KDM2B interactome using Cytoscape, categorized by Molecular Function as

847 annotated by DAVID.

848 (B) Gene Ontology analysis of KDM2B interactome shown as Biological Process.

849 (C) Schematic representation of the non-canonical PRC1.1 complex, including USP7. PRC1.1

850 preferentially binds to non-methylated CpG islands via the ZF-CxxC domain of KDM2B. The

851 ubiquitination of histone H2A on lysine 119 is mediated by RING1A/B. PRC1.1 can be recruited to

852 active genes in leukemic cells, indicated by H3K4me3.

853 (D) Identification of USP7 and other PRC1.1 proteins by LC-MS/MS in KDM2B-EGFP, PCGF1-EGFP and
854 EGFP-RING1B pull outs from nuclear extracts in K562 cells. The numbers indicate MS/MS counts for
855 each interacting protein corrected for expected peptides based on *in silico* digests (x10).
856 (E) Validation of USP7 and RING1B interactions as analysed by Western blot in canonical PRC1
857 (PCGF2/PCGF4/CBX2/RING1B) and non-canonical PRC1.1 (PCGF1/RING1B) pull outs. Input (I), non-
858 bound (NB) and bound (B) fractions are shown.
859

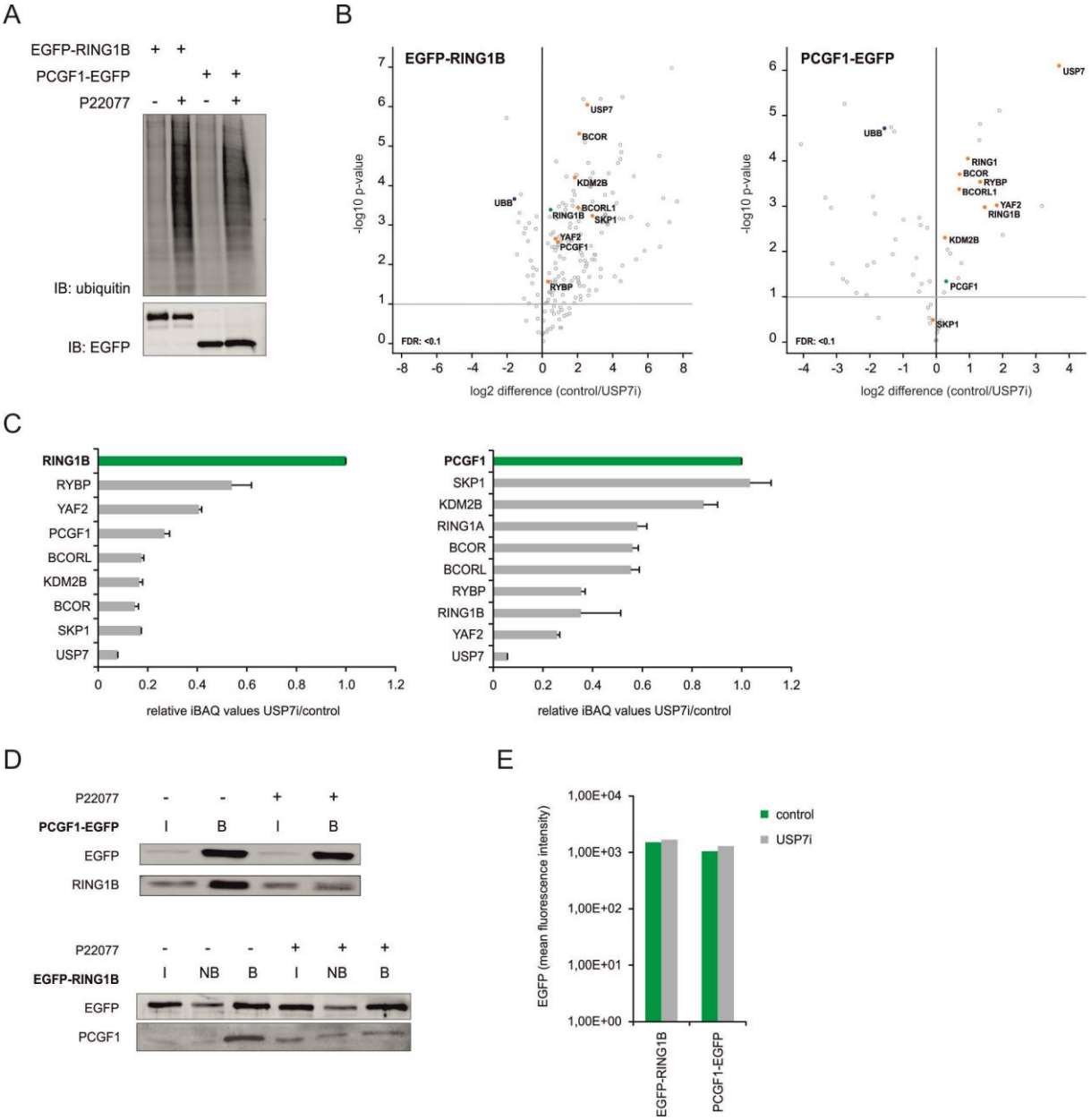


**Figure 2. USP7 is essential for PRC1.1 integrity**

(A) Purification of his-tagged ubiquitinated proteins under denaturing conditions in EGFP-RING1B and PCGF1-EGFP cells treated with DMSO (-) or P22077 (+) for 24h followed by Western blot analysis. (B) Label-free quantification (LFQ) intensities of EGFP pull outs on EGFP-RING1B (left) and PCGF1-EGFP (right) interactions in control (DMSO, 0.1%) and USP7i treated cells are illustrated as Volcano plot. The fold change difference (log2) of the EGFP pull out in control versus USP7i is plotted against the –log10 t-test p-value (y-axis). The bait protein (RING1B/PCGF1) is highlighted in green, PRC1.1 proteins in orange and UBB protein in purple.

869 (C) Intensity based absolute quantification (iBAQ) values for several identified PRC1.1 proteins are
870 shown in USP7i/control EGFP pull outs relative to RING1B (left) and PCGF1 (right). Data are shown as
871 mean ± SD (n=2 or 3).
872 (D) Western blot of EGFP pull outs on PCGF1-EGFP and EGFP-RING1B in the absence (-) or presence
873 (+) of P22077 for 72h probed with antibodies for EGFP, RING1B and PCGF1. Input (I), non-bound (NB)
874 and bound (B) fractions are shown.
875 (E) Mean fluorescent intensity (MFI) analysis of EGFP-RING1B and PCGF1-EGFP K562 cells in control
876 or USP7i treated cells at 72h.
877

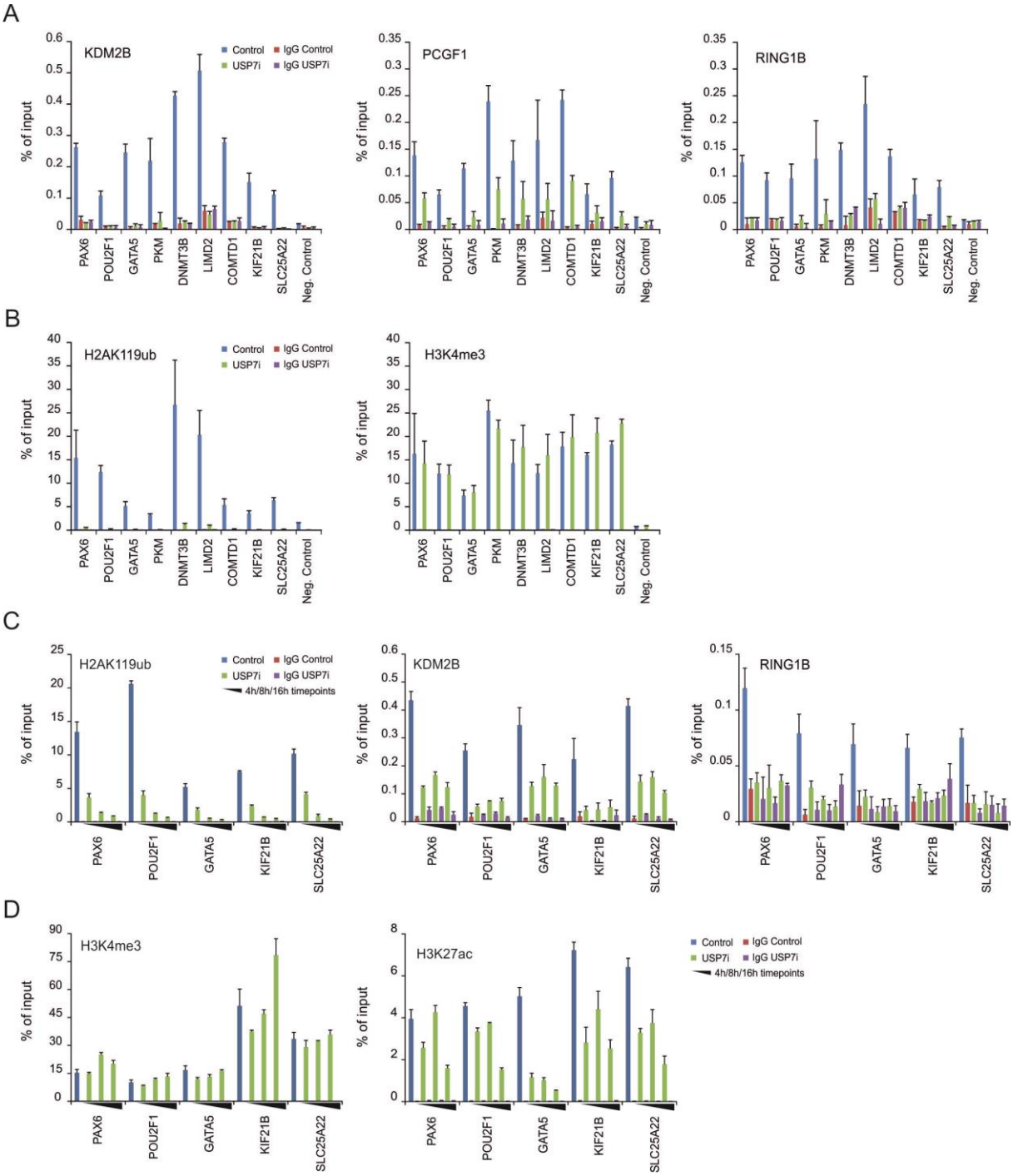


878

879

880 **Figure 3. Loss of PRC1.1 occupancy and H2AK119ub at target loci upon USP7 inhibition**

881 (A) ChIP-qPCRs on control or 72h P22077 (USP7i) treated K562 cells for endogenous KDM2B, PCGF1-

882 EGFP, EGFP-RING1B (B) H2AK119ub and H3K4me3 on several PRC1.1 loci previously identified by

883 ChIP-seq. Error bars represent SD of technical triplicates.

884 (C) ChIP-qPCRs on control or USP7i treated cells for 4h/8h/16h ( ) for H2AK119ub, KDM2B-

885 EGFP, EGFP-RING1B (D) H3K4me3 and H3K27ac on five PRC1.1 loci. Error bars represent SD of

886 technical triplicates.

887

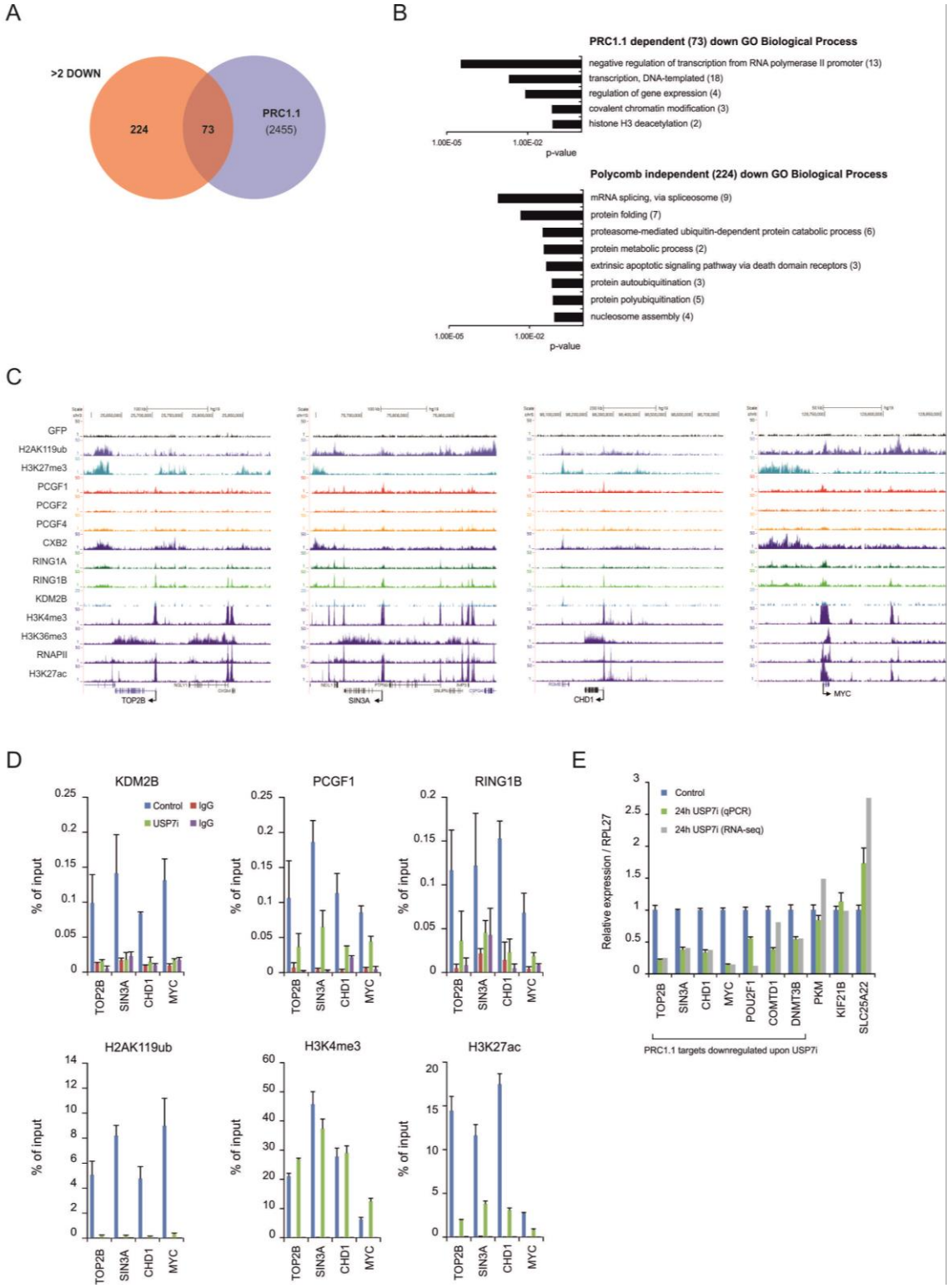


**Figure 4. USP7 inhibition leads to downregulation of a subset of PRC1.1 active target genes**

(A) Venn diagram showing overlap of genes downregulated by more than two fold after 24h of USP7 inhibition with previously identified PRC1.1 target genes.

893 (B) Gene Ontology analysis of downregulated genes identified as PRC1.1 targets (73) or Polycomb
894 independent targets (224) shown as Biological Process.
895 (C) ChIP-seq profiles of TOP2B, SIN3A, CHD1 and MYC as representative examples for PRC1.1 target
896 genes (73). Our ChIP-seq tracks are shown for GFP (control), H2AK119ub, H3K27me3, PCGF1, PCGF2,
897 PCGF4, CBX2, RING1A, RING1B and KDM2B. ChIP-seq tracks for H3K4me3, H3K36me3, RNAPII and
898 H3K27ac were downloaded from ENCODE/Broad.
899 (D) ChIP-qPCRs in control or 72h USP7i for KDM2B, PCGF1-EGFP, EGFP-RING1B and H2AK119ub or
900 16h USP7i for H3K4me3 and H3K27ac.
901 (E) Validation of relative gene expression levels of PRC1.1 target genes by qRT-PCR in control and
902 P22077 treated cells (24h). Data are represented as mean ± SD.
903

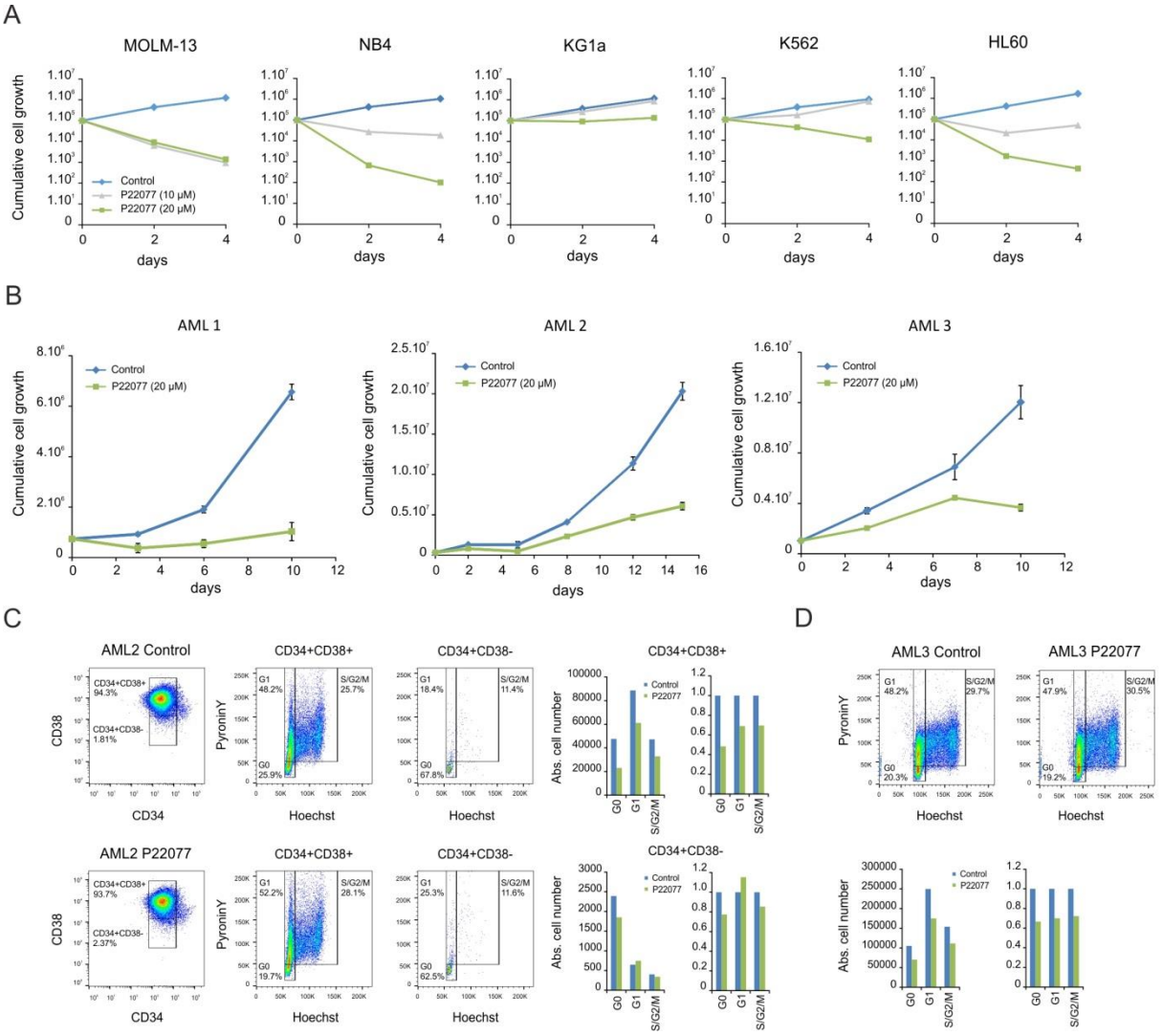


**Figure 5: Sensitiviy of primary AMLs towards USP7 inhibition**

(A) Cumulative cell growth of different AML cell lines in control (DMSO) or P22077 treated (10 µM and 20 µM) conditions.

(B) Cumulative cell growth of primary AML patient cells (n=3) grown on MS5 co-culture treated with DMSO (control) or P22077 (20 µM) performed in duplicate.

(C) Analysis of both cycling and quiescent AML cells by Hoechst/PyroninY stainings within the $CD34^+/CD38^+$ and $CD34^+/CD38^-$ populations (D) or whole population (AML3). Cells were treated with DMSO (control) or P22077 (20 µM) for 3 days while AMLs were grown on MS5 co-culture. Absolute cell numbers were calculated in $G_0$, $G_1$ and $S/G_2/M$ fractions.

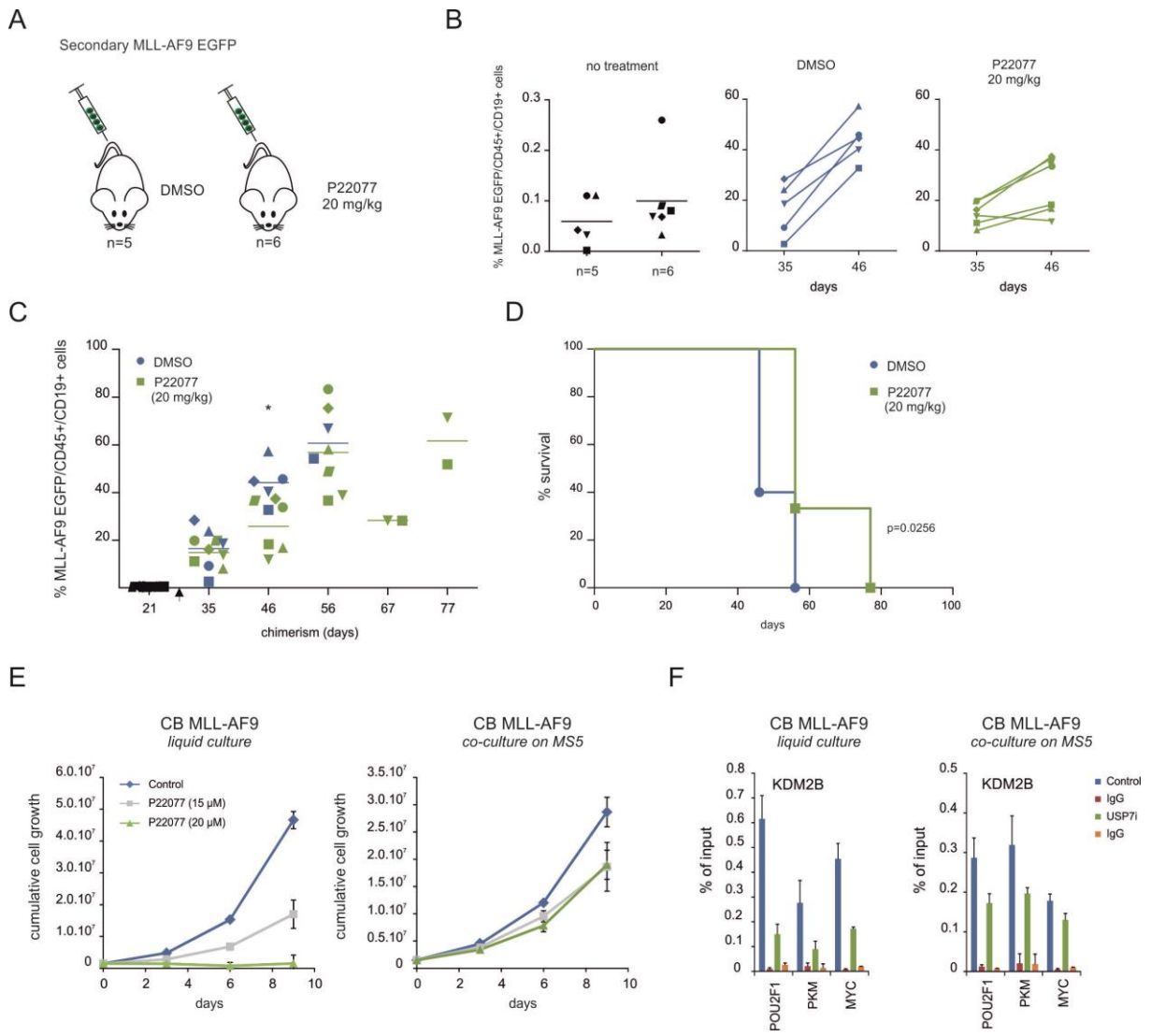


**Figure 6: Evaluation of USP7 inhibition in xenograft leukemia mouse model**

(A) Experimental setup of our human CB MLL-AF9 xenograft mouse model. Here 5 x $10^4$ MLL-AF9 EGFP cells from a primary leukemic mouse were IV injected into secondary recipients (n=11).

(B) Peripheral blood analysis of MLL-AF9 EGFP/CD45$^+$/CD19$^+$ cells, three weeks after injection prior to treatment (left) and 2.5 weeks following treatment (right). Mice were treated daily with either DMSO as control (n=5) or 20 mg/kg P22077 (n=6).

(C) Peripheral blood chimerism levels of control and P22077 (20 mg/kg) treated mice over the course of the experiment. Treatment was started at day 28 (4 weeks post-transplant) indicated with the arrow.

927 (D) Kaplan-Meier curve showing the survival of DMSO (n=5) and P22077 (n=6) treated mice.

928 Statistical analysis was performed using a log-rank test.

929 (E) Cumulative cell growth of CB MLL-AF9 cells grown under myeloid permissive conditions in liquid

930 and co-culture on MS5, treated with DMSO (control) or P22077 (15 and 20 µM).

931 (F) ChIP-qPCR for KDM2B in CB MLL-AF9 cells treated with DMSO or P22077 (48h) under either liquid

932 culture or MS5 co-culture conditions.

933

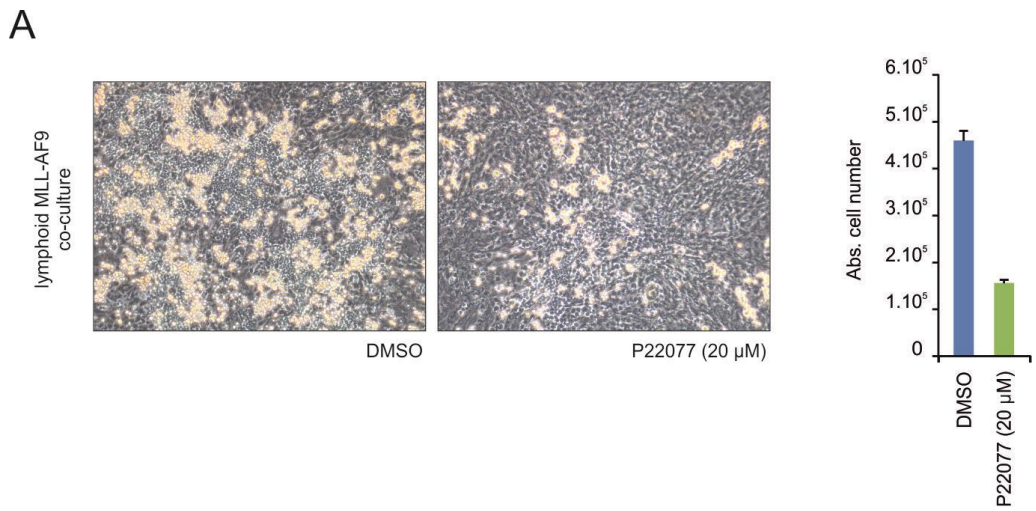


**Figure supplement 1. Sensitivity of lymphoid MLL-AF9 cells grown on MS5 for P22077**

(A) Lymphoid MLL-AF9 (GFP) co-culture on murine stromal cells treated with DMSO or P22077 (20 µM), day 6. Lymphoid MLL-AF9 cells typically form cobblestone areas (left). Absolute cell numbers corrected for human $CD45^+$ and $GFP^+$ are shown 10 days upon DMSO or P22077 (20 µm) treatment (right).